UNIVERSITY **POLITEHNICA** OF BUCHAREST
Faculty of Biotechnical Systems Engineering
Department of Biotechnical Systems

Eng. Bianca-Ștefania DRĂGOIU (ZĂBAVĂ)

Summary of PhD Thesis

RESEARCHES ON THE SETTLING PROCESS AND MECHANICAL WASTEWATER TREATMENT

Scientific supervisor:

Prof. Dr. Ing. Gheorghe VOICU

Bucharest (2020)

CONTENTS

FOREWORD

The paper is structured in 7 chapters, developed in 218 pages, contains 150 figures and graphs, 138 mathematical relations, 37 tables, as well as a reference list consisting of 226 references. Also, the paper includes a list of notations (4 pages), and at the end are presented a series of annexes (17 pages) that present materials and data related to the performed studies and research.

The main objective of the doctoral thesis was the realization of theoretical and experimental research on the process of mechanical wastewater treatment through the operation of settling / sedimentation and identification of the main variables involved in this process.

The doctoral thesis "***Research on the settling process and mechanical wastewater treatment***" presents a synthesis of experimental research conducted by the author on the process of settling and mechanical treatment of wastewater, respectively the CFD simulation of the settling process in view of its optimization.

In **Chapter 1**, entitled "*Introduction. The importance of wastewater treatment and purification. The objectives of the doctoral thesis*" are presented some aspects regarding the importance and the specific objectives through which the main objective can be achieved, approached both from a theoretical and experimental point of view.

In **Chapter 2**, "*Technical systems for wastewater treatment*", are presented very briefly the characteristics of wastewater, current regulations in the field of wastewater treatment and the main methods used in the treatment process. Also, there are presented the influencing factors in the liquid-solid separation in the clarifier, and the manner in which the use of coagulants influences the settling process.

In **Chapter 3**, "*Trends in the construction of clarifiers*", are presented theoretical notions on the settling process of solid impurities in wastewater, but also the construction of the main types of clarifiers. Several constructive variants of equipment used in the wastewater settling process, such as longitudinal, radial, vertical and lamellar settlers, are reviewed.

Chapter 4, "*Current state of research on the process of wastewater settling*" presents the basic principle of the settling process of wastewater sediments, the ideal model of clarifier, but also the balance of materials in the settling operation. There are presentef the results of theoretical and experimental research, conducted worldwide, on the influence of various factors on the efficiency of the settling process (solid particle concentration, construction factors and temperature), as well as the mathematical models proposed to study the process of wastewater purification by settling, derived from the theoretical and experimental studies of various researchers. At the end of the chapter are presented some conclusions on the importance of the settling process and the recommendations of the specialists on the purification process by settling, based on the influence of the process factors derived from the specialized studies.

In **Chapter 5**, "*Theoretical aspects and contributions on the process of wastewater purification by settling*" are presented: an algorithm and calculation program for determining the position of the critical point of the clarification curve at settling in stationary column; the mathematical modeling of the wastewater settling process, by dimensional analysis, using the Π theorem, in view of the prediction of the settling rate of solid particles in wastewater, taking into account a number of 7 main parameters that influence the process; CFD numerical simulation of the settling process on two constructive variants of radial clarifiers (decanters), in order to optimize the process, by analyzing the 2D flow, aiming to study the flow of the liquid-solid mixture inside a radial clarifier, in the feeding area, using the Ansys Fluent program. Two simulations were performed under identical conditions: one for a clarifier with a feeding pipe having a constant diameter of 1 m over its entire height, respectively one for a clarifier with a feeding pipe in the form of a funnel, with a diameter of 1 m up to 3.5 m height, after which the feeding pipe flares and reaches a diameter of 2 m at water discharge in the clarifier. At the end of the chapter are presented some synthetic conclusions resulting from the performed theoretical studies.

Chapter 6, “*Experimental research on the wastewater treatment process by settling*”, comprises the results of own experimental research, carried out both in the laboratories within the Faculty of Biotechnical Systems Engineering, UPB, and in-situ, in two urban wastewater treatment plants located in different areas of the country. The research carried out in the laboratory aimed at: determining the influence of solid particles concentration, for three types of liquid-solid mixture, on the settling rate; calculation of the settling rate of these liquid-solid mixtures, based on Stokes' law, previously determining experimentally the particle density, and the density and viscosity of the suspension; determining the turbidity of the liquid-solid mixture at the height of the settling column, by means of standard samples of known concentrations, for different concentrations of the liquid-solid mixture; determining the influence of the size and concentration of solid particles on the settling process for three types of liquid-solid mixture using the UV-VIS spectrophotometer, by determining the variation of the absorbance over time; determining the clarification curve of an aqueous suspension of solid particles, using the intelligent Raspberry Pi system, by determining the turbidity using the VL53L0X turbidity sensor, but also the settling rate by image processing method of the interface between the clarified area and the general suspension area; determining the influence of coagulants on the settling process. Experimental research conducted in situ, in two urban wastewater treatment plants, consisted in determining the efficiency of a radial primary clarifier based on the concentration of solid particles at the inlet and outlet of water from the clarifier, as well as experimental determinations on the removal of coarse waste from wastewater by mechanical methods and their recovery in the form of briquettes at one of the wastewater treatment plants. In-situ research continued with determinations on the amount of coarse impurities generated at different times of the year and the total suspended solids content of the influent and effluent, for the same periods of the year at the second wastewater treatment plant. In this chapter, the apparatus, working equipment and some stands used for experimental research were presented. At the end of the chapter are presented the synthetic conclusions on the experimental determinations made on the settling process of liquid-solid mixtures and mechanical wastewater treatment.

Chapter 7, “*Final Conclusions. Personal contributions. Perspectives for future research*” presents the general conclusions that emerge from the theoretical studies and experimental research conducted on the process of settling and mechanical wastewater treatment.

Also, the personal contributions of the author on the studied phenomena and the experimental research conducted within the doctoral thesis are presented. New research directions are presented, which may be the subject of theoretical studies and experimental research to be approached in the future by other researchers.

The author considers that the present doctoral thesis represents a minimal contribution to the clarification of some aspects related to the settling process of and mechanical wastewater treatment, which can be deepened in further research.

LIST OF SYMBOLS, ABBREVIATIONS AND NOTATIONS

Chapter 2 – Technical systems for wastewater treatment

l.e	equivalent inhabitants
d_{ech}	equivalent diameter of particle (m)
V	volume of the sphere (m^3)

Chapter 3 – Trends in the construction of clarifiers

Q	water flow (m^3/s)
B	clarifier width (m)
L	clarifier lenght (decanter) (m)

Chapter 4 – Current state of research on the process of wastewater settling

G	particle weight (N)
v_p	particle settling (sedimentation) rate (velocity) (m/s)
ρ_l	fluid density (kg/m^3)
ρ_p	solid particle density (kg/m^3)
φ_1	particle sphericity factor (-)

Chapter 5 – Theoretical aspects and contributions on the process of wastewater purification by settling

DI	matrix containing the experimental data
C	height of the critical point of settling (m)
L, *M*, *T*	fundamental quantities: length, mass, time
CFD	computational fluid dynamics

Chapter 6 – Experimental research on the wastewater treatment process by settling

E	separation efficiency (%)
MTS	total content of suspended matter (mg/L)
R^2	correlation factor (-)

CHAPTER 1. INTRODUCTION. THE IMPORTANCE OF WASTEWATER TREATMENT AND PURIFICATION. THE OBJECTIVES OF THE DOCTORAL THESIS

1.1. Introduction

The availability of a clean and safe source of water is essential for human health and welfare, as well as for agriculture, industry and transport, [220]. The main method of combating water pollution, and a means of improving wastewater quality, is the wastewater treatment process, which is currently the most widely used process, [186].

1.3. The objectives of the doctoral thesis

In the present context, the general objective of the doctoral thesis was to conduct theoretical and experimental researches regarding the mechanical wastewater treatment process through the operation of settling / sedimentation and to identify the main variables involved in this process. In order to fulfill the general objective of the thesis, it was necessary to achieve the following specific objectives, according to Fig. 1.4.

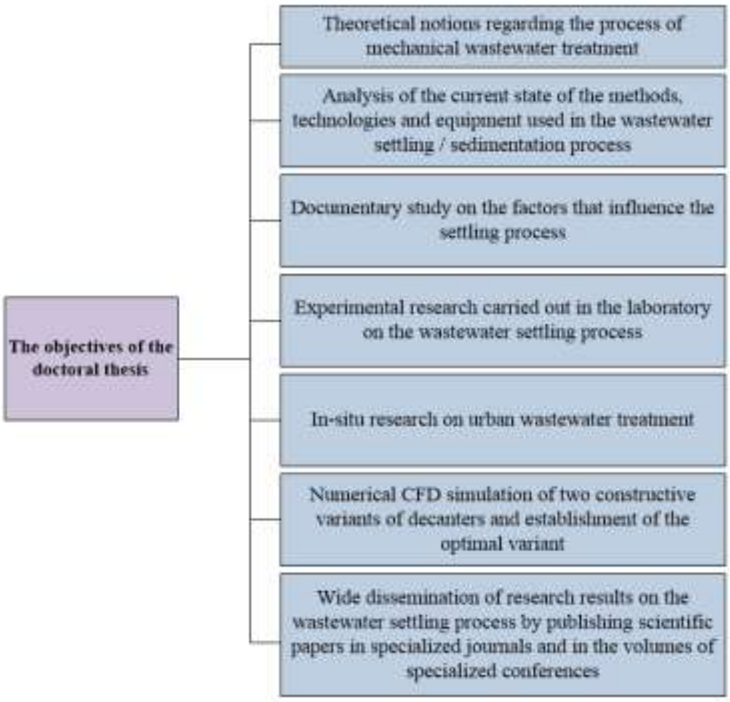

Fig. 1.4. The specific objectives of the doctoral thesis

CHAPTER 2. TECHNICAL SYSTEMS FOR WASTEWATER TREATMENT

2.1. Characteristics of wastewater and its components

The characteristics and composition of wastewater mostly determine the structure and dimensions of a treatment plant. These are established by laboratory analysis, which determine the quantity and the condition of any kind of materials in the water. By taking samples from different points of the wastewater treatment plants, the efficiency of the treatment process of the plants can be established. The doctoral thesis presents the physical, chemical and biological characteristics of wastewater.

2.2. Current regulations in the field of wastewater treatment

The main objective of European Union (EU) policy in the field of water is the guarantee of availability, throughout the EU, of a sufficient amount of good quality water, so that to cover the needs of the population and the environment.

The national authority "Romanian Waters" is the organization responsible for the Integrated Water Monitoring System in Romania (IWMSR) and specific databases.

2.3. Wastewater treatment methods

Wastewater treatment is a basic method for the protection and reuse of water resources, clearly demonstrated by the consequences of its implementation in many countries around the world. In a wastewater treatment plant can be distinguished a primary (mechanical) stage, a secondary (biological) stage and, in some plants, a tertiary stage (biological, mechanical or chemical).

The first stage in the wastewater treatment process is the primary treatment, also called *mechanical treatment*. Thus, at the entrance to the treatment plant, takes place a process of retention of coarse impurities, using screens and sieves, which have the role of retaining the impurities that could clog the pipes or damage the equipment. Further, water passes through special equipment which retains smaller particles, such as sand and fine grit. The next step in a wastewater treatment plant is the removal of grease, followed by the removal of fine particles in primary clarifiers. All fine solid particles accumulated in the primary clarifiers are called primary sludge, [216].

The secondary stage of wastewater treatment, also called *biological treatment,* removes about 85% of the organic matter present in water, and the advanced wastewater treatment known as *tertiary treatment* is introduced into the treatment technology when it is necessary to obtain superior water quality, which is impossible to achieve through the secondary treatment processes.

2.4. Factors of influence in liquid-solid separation in the clarifier

The separation process of liquid-solid mixture is influenced by many factors related to both the solid and liquid components, as well as the construction parameters of the clarifier.

2.4.1. Factors related to the solid component

These factors refer to: *the influence of particle size* - settling tank, the coarse particles tend to settle on the clarifier bottom and acquire a downward movement, while the fine particles tend to be entrained in the overflow current, [11]; *the influence of particle shape* - a spherical particle, considered ideal, will settle more easily than a particle that has an irregular shape, [48]; *the influence of solid suspensions concentration* - McNown et al. showed in their researches that an increase in the particles concentration results in a reduction of particles settling rate, [85]; *the influence of particle density* - high density particles tend to move directly to the lower area of the clarifier, while low density particles have a slight tendency to float and are attracted to the overflow current.

2.4.2. Factors related to the liquid phase of the mixture

The separation process of liquid-solid mixture is influenced by factors related to the liquid component such as: *water temperature* - Hazen [58], stated that "a given settling tank will work twice as much in summer as in winter"; *water density* - depends on the temperature and varies with the concentration of total solids in the wastewater, [42]; *water viscosity* - tends to decrease with increasing water temperature, [60]; *settling tank currents* - the recommended ratio between depth and diameter or decanter length is about 1/20, [209].

2.4.3. Factors related to the constructive parameters of the clarifiers

In the doctoral thesis are presented factors that refer to: *the influence of the uniformity of the water current distribution* - the shape of the tank and the mode of inlet and discharge of water from the clarifier are major factors influencing the flow in a settling tank, [144]; *the influence of the settling tank shape* - in the case of longitudinal clarifiers, a uniform flow with less turbulence can be obtained over a large part of the tank, [58]; *the influence of scraping and sludge removal equipment; the influence of water inlet and outlet area from clarifier* - Rostami et al. [120] showed that the number of spillways improve flow uniformity and decrease the dimension of crossing area; *the influence of the baffles in clarifiers* - placing a baffle in the close proximity of the wastewater intake area in the clarifier is the most efficient solution, [111].

2.5. Use of coagulants in the settling process

By settling, very fine and colloidal (particles smaller than 1μm) suspensions cannot be removed from wastewater, no matter how long the process would take. Researches in the field support the idea that the efficiency of the settling process is improved when coagulants are used, [10, 54].

2.6. Conclusions

Researches conducted worldwide have shown that particles with a sphericity factor of 0.85 had an average settling rate twice as high as that observed for particles with a sphericity factor of 0.35. However, it has been established that a temperature difference of only 1 ^{0}C is sufficient to cause a decrease in settling efficiency and that rapid changes in density due to temperature, solids concentration or salinity can induce density currents that can cause dead zones and low efficiency in horizontal tanks.

Also, it has been shown that the presence of a vertical deflector in the inlet area of the settling tank increased the efficiency of solid particles removal from 90.4% to 98.6% . At the same time, from the studies performed on the settling process, it was highlighted that solid particles with dimensions smaller than 1μm can be removed with the help of coagulants, thus improving the efficiency of the settling process.

CHAPTER 3. TRENDS IN THE CONSTRUCTION OF CLARIFIERS

3.1. The process of settling of solid impurities in wastewater

The most common method of mechanical treatment (primary) is smooth settling (conventional). This is an effective method of removing suspended solids from wastewater, and the separation takesplace by gravitational force.

3.2. Construction of settling (sedimentation) tanks

All settling tanks can be divided into four zones, each with a specific function. These areas are: the inlet zone (raw water inlet), the settling zone, the outlet zone (clarified water discharge) and the sludge storage zone (located on the equipment bottom).

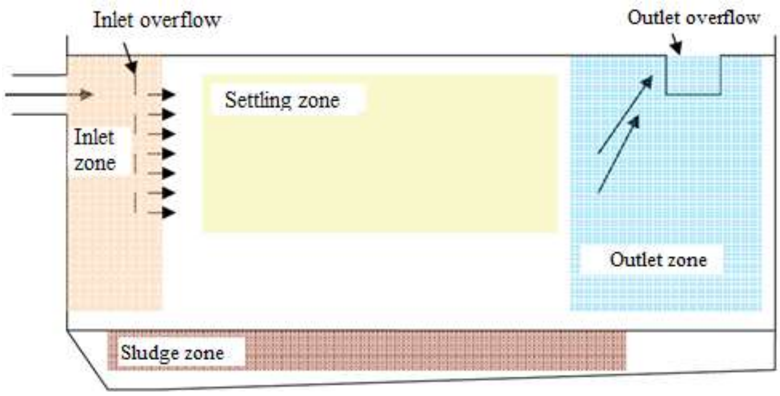

Fig. 3.5. Positioning zones in a horizontal settling tank, [128]

3.3. Constructive solutions of clarifiers

Primary clarifiers are open tanks that have the role of retaining decantable particles or those brought in decantable form, with dimensions smaller than 0.2 mm, which have not been retained in grit removal equipments. By the flow direction of the wastewater stream, primary clarifiers are classified into longitudinal, radial, vertical and inclined (lamellar) clarifiers, the most common in practice being the longitudinal and radial ones. An example of a *radial clarifier* is shown in fig. 3.8.

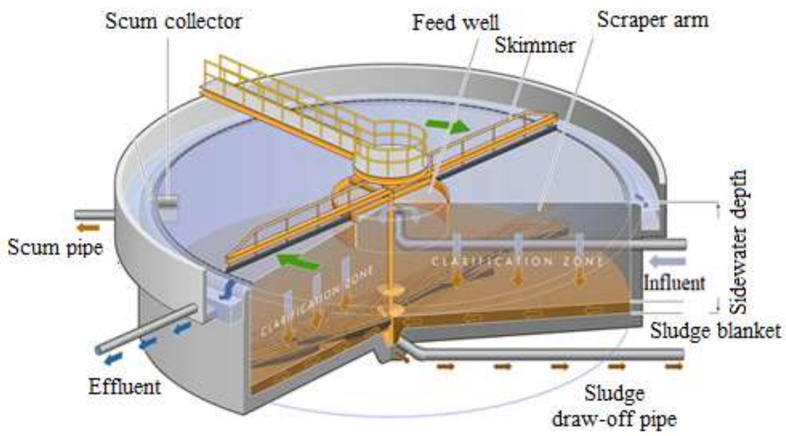

Fig. 3.8. Constructive scheme of a radial clarifier, [155]

The stream of raw wastewater enters through the center of the clarifier, moves radially in all directions, and during the movement of the water the suspensions from the wastewater stream settle on the tank bottom, the clarified water being captured by discharge into a peripheral gutter located at the water mirror, from where it is discharged from the installation. The slope of the conical clarifier area is usually from 1:10 to 1:12 and depends on the type of sludge collection mechanism. The diameter of the tank varies from 3 meters to over 100 meters, [102].

Longitudinal clarifiers are tanks with a rectangular section, in which the raw wastewater enters at a low flow at one end, during transition along the length of the tank the decantable solids from the wastewater stream settle on the bottom, and at the other end the stream of clarified water containing dissolved matter is discharged into a gutter located at the water mirror, from where it is discharged to the biological treatment stage.

3.4. Conclusions on the process and construction of clarifiers

The efficiency of solids removal depends on the characteristics of the clarifier. Sedimentation equipment that include deflectors in the intake area for energy dissipation, a resting area for the settling particle, mechanical devices for removing decanted solids and a reduced velocity of clarified water at the outlet, is commonly referred to as a "clarifier (decanter)".

The terms sedimentation and settling are used interchangeably. A sedimentation tank can also be called a sedimentation basin or settling tank. Sedimentation tanks can have different shapes and can only function as a settling tank or can also incorporate sludge flocculation and compression. Different own models are available, but the basic functioning of all types is similar.

CHAPTER 4. CURRENT STATE OF RESEARCH ON THE PROCESS OF WASTEWATER SETTLING

4.1. The basic principle of the sediment settling process in wastewater

Through the settling process, the sedimentation rate of a particle increases until the settling force (the particle's own weight) becomes equal to the resisting forces. In this case, there is a balance between the forces acting on the particle, for which (dvp/dt) = 0. Particles weight G, Archimedes force F_A and viscous resistance F_R act on spherical particles isolated from the fluid (fig. 4.1).

In the steady state of the force system, the sedimentation rate of the particles can be evaluated according to the following Figure, [107]:

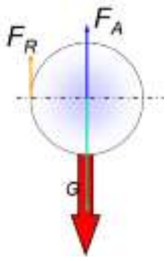

Fig. 4.1. The system of forces acting on the solid particle in the suspension, [46]

Following the simplifications results *Stokes' relation* for the sedimentation rate calculation by static settling of the solid particles of impurities in the conditions of the laminar flow:

$$v_p = \frac{(\rho_p - \rho_l) \cdot d^2 \cdot g}{18\eta} \qquad (4.5)$$

For sedimentation of particles other than spherical, the expression is corrected by a sphericity factor φ_1.

4.4. Synthesis of worldwide research on the process of wastewater purification by settling

4.4.1. Mathematical models proposed for the process of wastewater purification by settling

Numerical studies have been and continue to be performed in a number of sedimentation (settling) tanks used in water treatment plants. These models have been gradually improved since Larsen (1977), [75].

Marcos Von Sperling proposed the following formula for viscosity (m^2/s) as a function of temperature, [140]:

$$\eta = 3.76 \cdot 10^{-6} \cdot T^{-0.450} \qquad (4.35)$$

where T – temperature, (ºC).

Considering the sedimentation rate equation given by Stokes' law, it appears that the sedimentation rate depends on the temperature.

A number of other mathematical models have been reported in the literature [20,51,55,56,63,94,95,146].

4.4.2. The current state of experimental research on the process of wastewater treatment by settling

The synthetic analysis of these works aimed to study the process of solid particles removal from the liquid-solid mixture by settling through the influencing factors.

In paper [145], the authors plotted the clarification curves for six samples of different concentrations (1.37 g/L, 2.37 g/L, 3.42 g/L, 4.10 g/L, 5.46 g/L, respectively 6.83 g/L) by measuring the clear water / suspension interface over time, for 45 min. It was obtained that the settling rate decreased at higher concentrations of solid particles, because each particle will be more and more disturbed by the surrounding particles, thus decreasing the settling rate.

In 2010, Podoleanu C.E. carried out experimental research on the settling process, in terms of the concentration of solid particles in the longitudinal settling tank, [100].

To identify the concentration distribution in the clarifier, measurements were performed to determine the concentration (C1 – C6), on the length L (m) and the depth of the settling tank H (m). The author noted that in the first half of the settling tank is an intensification of sedimentation processes.

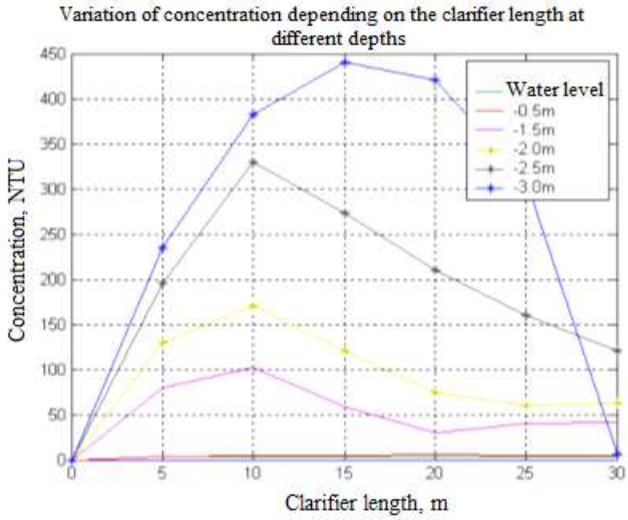

Fig. 4.11. Variation of concentration depending on the clarifier length at different depths, [100,166]

In another study, researches were carried out on the settling process for three constructive types, with distinct flow values (3 m^3/h, 4 m^3/h, 5 m^3/h și 8 m^3/h) and temperatures (100 °C, 85-90 °C și 75 °C), [168,171]. The authors observed that regardless the flow and temperature of the water subjected to decantation, the clarifier with a deflector plate has the best efficiency.

A. Razmi et al., in paper [111], (2009), studied the effect of baffle presence in the clarifier. Experimental researches had shown that the performance of the settling tank can be improved by changing tank geometry, which leads to a different distribution of velocities and flow patterns, and by placing the baffle near the water feeding area (s/L= 0.125), the optimal type was obtained.

Tarpagkou R. et al., (2013) studied the influence of temperature on the efficiency of the settling process, in two cases, namely: low temperatures (during winter) and high temperatures (during summer), [139]. The efficiency of the settling tank in the second case was around 80%, at low temperatures it reached 50%.

Another study was conducted to determine the influence of the temperature on the performance of sedimentation tanks and showed that water temperature visibly affects the settling rates by fluid viscosity, [73]. At 29 °C temperature, a sedimentation rate of 1.5 m/h was obtained, while for 11 °C temperature, the sedimentation rate decreased to 0.95 m/h, for a concentration of solid particles of 60 mg/mL.

4.5. Conclusions on the synthesis of research on the settling process

Sedimentation is of particular importance in wastewater treatment, and the settling tanks can account for as much as 30% of the total investment in a treatment plant.

The analyzed scientific papers showed that the process of the liquid-solid mixture separation is influenced by numerous factors related to both the solid component, the liquid component and the constructive factors of the clarifier.

Wastewater temperature has been found to play an important role in the settling process. Experimental results showed that at low water temperatures, the efficiency of the sedimentation process decreases, water viscosity increases, the forward resistance of solid particles increases and as a result, the sedimentation rate decreases.

According to worldwide researches, in order to improve the efficiency of the settling process, the following may be recommended: mounting a spillway in the water discharge area from the clarifier, the use of tangential clarifiers, equipped with a spillway and scraping devices for sludge evacuation, in order to avoid the formation of the circulation area, which is known as the dead zone in the clarifier, it is recommended to mount a baffle inside the clarifier and position it correctly to improve the performance of the clarifier, but also to cover the clarifier with a protective foil, in winter, to increase the temperature of the wastewater.

CHAPTER 5. THEORETICAL ASPECTS AND CONTRIBUTIONS ON THE PROCESS OF WASTEWATER PURIFICATION BY SETTLING

5.2. Algorithm and calculation program for determining the position of the critical point of the clarification curve at the sedimentation of solid particles in stationary column

The critical point of a clarification curve represents its intersection point with the variation curve of the sludge height in compaction and corresponds to the moment when clear water – suspensions and suspension - compacted sludge interfaces overlap, and in the column in which the sedimentation process takes place there are only two areas left: one of clarified water and one of compaction sludge, that means that the clarification process has ended.

For these experimental determinations, a laboratory stand for the study of sedimentation (W2 - Armfield, UK) was used, using an aqueous suspension of calcium carbonate particles with an initial concentration of 8%.

Fig. 5.2. Appearance of column with suspension during the experiment, [124]

Only the positions of the *clear water - aqueous suspension of solid particles* interface were recorded for a period of 24 hours, as follows: every 6 minutes for the first 1.5 hours of the experiment, then every hour for up to 6 hours and at 24 hours.

The program for determining the critical point position, if the critical point position is estimated by the graphical method, was developed based on a sequential algorithm whose structural scheme is found in fig. 5.3.

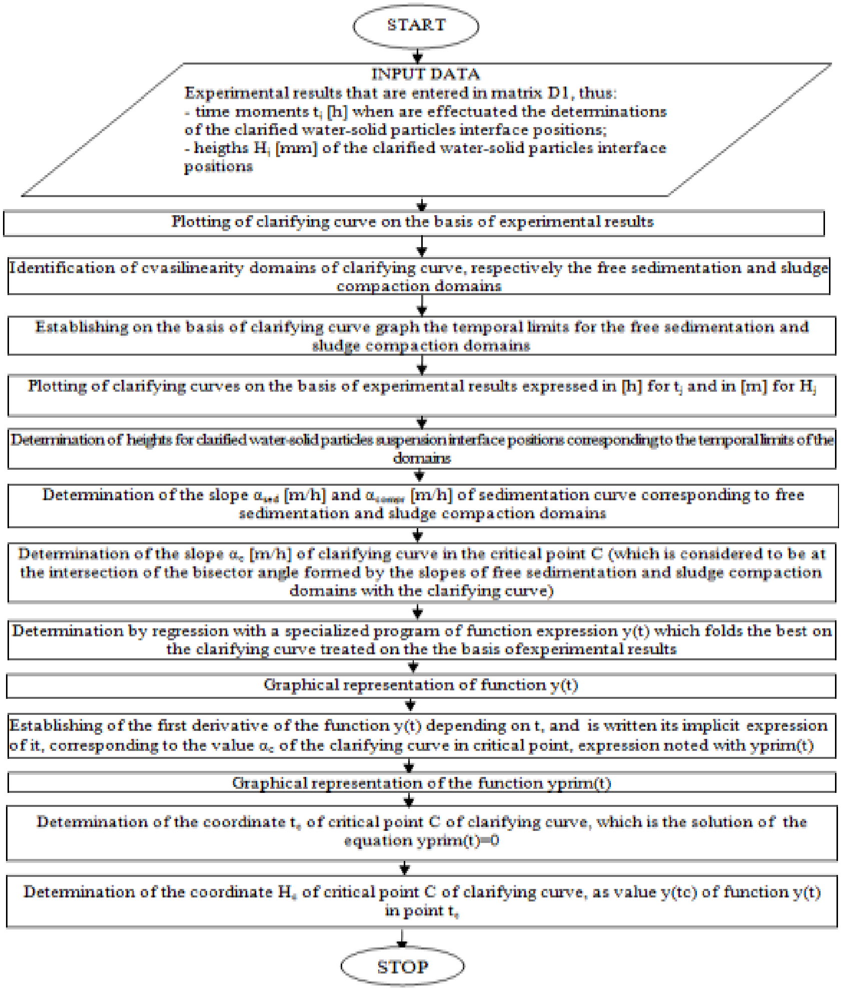

Fig. 5.3. Structural scheme of the sequential algorithm for determining the critical point,[124]

The experimental results were entered in the DI input data matrix, as follows:

- on the line 0 of DI matrix are mentioned the time moments t_j [h] at which are recorded the determinations of clarified water - suspension of solid particles interface positions, noted with $DI_{0,j}$;

- on the line 1 of DI matrix are noted heights H_j [mm] of clarified water - suspension of solid particles interface positions noted with cu $DI_{1,j}$;

where j represents the current number of the determination being performed and whose maximum value corresponds to the number of matrices columns DI.

$$j = 0..21$$

$$DI = \begin{pmatrix} 0 & 0.1 & 0.2 & 0.3 & 0.4 & 0.5 & 0.6 & 0.7 & 0.8 & 0.9 & 1 & 1.1 & 1.2 & 1.3 & 1.4 & 1.5 & 2 & 3 & 4 & 5 & 6 & 24 \\ 790 & 756 & 731 & 708 & 686 & 665 & 646 & 627 & 609 & 591 & 574 & 557 & 543 & 527 & 512 & 497 & 418 & 305 & 229 & 198 & 190 & 167 \end{pmatrix}$$

By running the program it was found that the corresponding time to the critical point of the clarification curve has a value of 3.39 hours. The height of the clear water - sludge in compaction interface position H_C (m), corresponding to the critical point is the value of the function y(t) at the time t_C, the value obtained for this being 0.268 m.

5.3. Mathematical modeling of the wastewater settling process, through dimensional analysis, using the Π theorem

Dimensional analysis remains one of the most powerful approaches to solving physical problems, [15]. Dimensional analysis is based on the extremely simple, clearly intuitive fundamental idea, but: physical laws do not depend on the basic units of measurement arbitrarily chosen. Despite its simplicity, dimensional analysis allows to obtain remarkably profound results, including progress in theories of gravity and turbulence, [87].

In order to anticipate the settling rate of solid particles in wastewater, the theory of dimensional analysis was applied for the mathematical modeling of the process, based on the π theorem, stated by Buckingham [21] and described in detail in [133].

The steps required to apply the theorem are:

- determining all the parameters that influence the phenomenon;
- the expression of an indeterminate function that contains the *n* parameters, in *n* being included the phenomenon $f(a_1, a_2, a_3 ... a_n) = 0$;
- dimensional equations are written for each parameter:

$$[a_1] = ...;\quad [a_2] = ...;\quad [a_n] = ...;$$

and the number of fundamental physical sizes involved in that phenomenon is determined.

- there are formed (*n-m*) adimensional groups which each contain *m* + 1 terms, *m* being the number of fundamental physical sizes.

Based on theoretical and experimental researches of the wastewater settling process, a number of 7 main parameters that influence the sedimentation process were considered in the study:

- wastewater flow, Q (m^3/s);
- clarifier length, h (m);
- settling rate, v_s (m/s);
- particle diameter, d (m);
- the kinematic viscosity of the liquid, ν (m^2/s);
- water stationary time in the clarifier, t (s);
- particle density, ρ_p (kg/m^3).

The default function, which describes dimensionally the settling process, where all terms in relation to the fundamental sizes in SI (L, M, T) are homogeneous dimensional is:

$$f(Q, h, v_s, d, \nu, t, \rho_p) = 0 \tag{5.1}$$

n = 7 main parameters that influence the settling process;

m = fundamental physical sizes (h, d, t);

n - m = 4 (4 adimensional groups are formed that each contain m + 1 terms).

Case A:

Considering as determining sizes the group (v_s, d, ρ_p), based on the π theorem adimensional compounds were determined (similarity criteria) of the settling process.

- physical directories sizes are Q (m^3/s), h (m), ν (m^2/s) and t (s)
- the determining sizes are v_s [m/s], d [m], ρ_p [kg/m^3]

$$f(Q, h, v_s, d, \nu, t, \rho_p) = 0$$
$$n = 7\ (Q, h, v_s, d, \nu, t, \rho_p) \quad (5.2)$$

For the directing physical sizes, the adimensional compounds have the form:

$$\pi_1 = v_s^{x1} \cdot d^{y1} \cdot \rho_p^{z1} \cdot Q \quad (5.3)$$
$$\pi_2 = v_s^{x2} \cdot d^{y2} \cdot \rho_p^{z2} \cdot h \quad (5.4)$$
$$\pi_3 = v_s^{x3} \cdot d^{y3} \cdot \rho_p^{z3} \cdot \nu \quad (5.5)$$
$$\pi_4 = v_s^{x4} \cdot d^{y4} \cdot \rho_p^{z4} \cdot t \quad (5.6)$$

Next, were determined the size of each group in which the exponents $x_1, y_1, z_1; x_2, y_2, z_2; x_3, y_3, z_3$ and x_4, y_4, z_4 can be determined from the conditions that π_1, π_2, π_3 și π_4 are adimensional, in relation to the fundamental quantities L (length), M (mass), T (time).

Assuming that π_1, π_2, π_3 and π_4 are adimensional, in relation to the three fundamental quantities L, M, T, the exponents are further determined, then they are replaced in the expression of the adimensional group.

For a first approximation, the mathematical model of the product of powers of the other adimensional sizes was proposed, resulting that the settling rate has the calculation form:

$$v_s^2 = \frac{Q}{d^2 \cdot k_1 \cdot \left(\frac{h}{d}\right)^a \cdot \left(\frac{1}{Re}\right)^b \cdot \left(\frac{t}{d}\right)^c} \ (m/s) \quad (5.21)$$

where: k1, a, b, c are constant coefficients, respectively exponents calculated by linear regression based on experimental data.

Case B:

Considering as determining sizes the group (v_s, h, ρ_p), based on the π theorem adimensional compounds were determined (similarity criteria) of the settling process:

- physical directories sizes are Q (m^3/s), d (m), ν (m^2/s) și t (s);
- the determining sizes are v_s (m/s), h (m), ρ_p (kg/m^3);
- the expressions of the 4 adimensional groups are written.

Following the same steps as in case A, it was obtained that the settling rate can be written as:

$$v_s^2 = \frac{Q}{h^2 \cdot k_1 \cdot \left(\frac{d}{h}\right)^a \cdot \left(\frac{\nu}{v_s \cdot h}\right)^b \cdot \left(\frac{t}{d}\right)^c} \ (m/s) \quad (5.34)$$

5.4. Numerical CFD simulation of the settling process

The aim of this study was to simulate the flow of a liquid-solid mixture inside a radial decanter, in the feeding area, by analyzing the 2D flow, using the Ansys Fluent program.

Two simulations were performed under identical conditions: one for a wastewater feeding pipe with a constant diameter of 1 m over the entire height of 5.5 m, and another with a feeding pipe with a diameter of 1 m up to 3.5 m height, after which it flows out and reaches a diameter of 2 m when the water is discharged into the decanter (similar to a funnel).

Fig. 5.10. Isometric view of a radial clarifier in a simplified structure in the case of a clarifier with a feeding pipe of constant diameter (a) or flared (b)

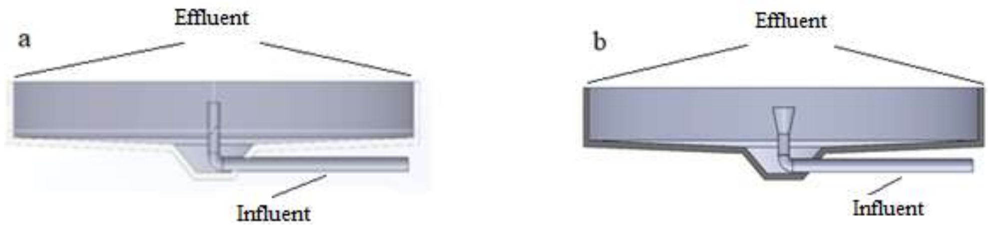

Fig. 5.11. Section in the central area of the clarifier with a feeding pipe with a constant diameter of 1 m (a), respectively flared reaching a diameter of 2 m (b)

The geometric models were made in the "Design Modeler" module and are presented in fig. 5.12a and 5.12b.

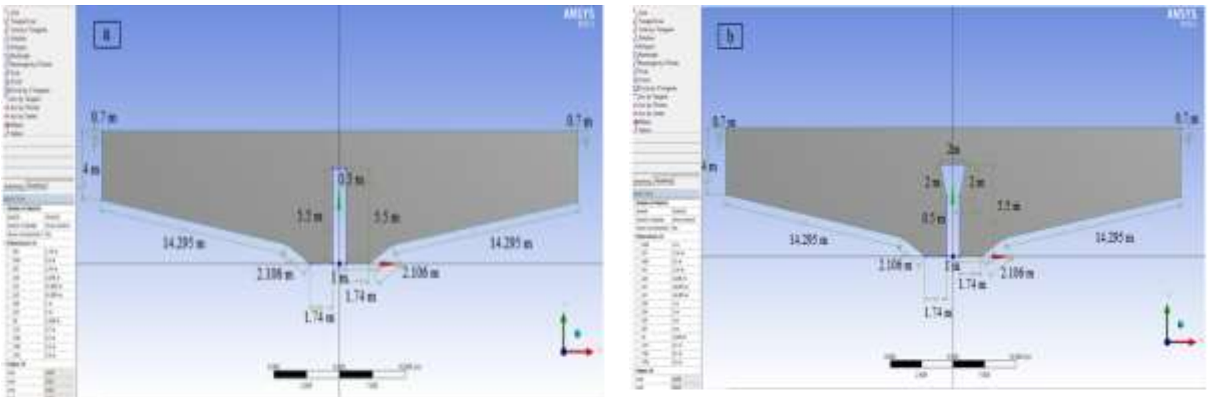

Fig. 5.12. Geometric model performed for the analysis of the clarifier with a feeding pipe with a constant diameter of 1 m (a) and for a 2 m pipe in the feeding area (b)

Below are the results obtained at 60 s, 120 s and 180 s (simulation time) for velocity, Reynolds number in each cell and turbulence intensity for the two analyzed clarifiers.

a. Fluid velocity for the clarifier with the feeding pipe of 1 m

Figure 5.18 shows the distribution of velocity for the clarifier with a feeding pipe of 1 m, to 60 s, 120 s and 180 s, and details of the feeding in the same time intervals. It can be observed, although the velocity in the feeding area has been set to 0.036 m/s, there are areas in the clarifier where the velocity can reach 0.103 m/s and that the maximum values are obtained in the feeding area.

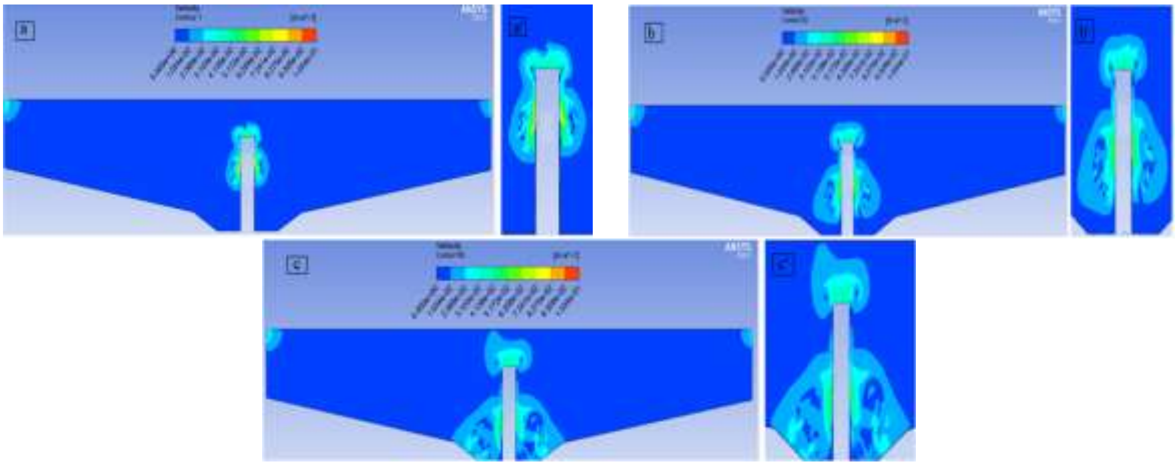

Fig. 5.18. Velocity distribution for the clarifier with 1 m feeding pipe at 60 s (a), 120 s (b) and 180 s (c), respectively details in the feeding area, in the same time intervals (a'-c ')

According to Fig. 5.18, it can be seen that the direction of travel is generally towards the bottom of the clarifier (largely due to the vortices that are created at the end of the pipe), where there is a considerable pressure difference in the fluid mass.

b. Reynolds number for the clarifier with 1 m feeding pipe

Figure 5.20 shows the distribution of the Reynolds number along the length of the geometric model for the clarifier with the feeding pipe of 1 m, at 60 s, 120 s and 180 s, respectively details from the feeding area, in the same time intervals. The maximum values reached by the Reynolds number on the clarifier length are 14.7 for t = 60 s 39.6 for t = 120 s and 53 for t = 180 s. The appearance of eddies also determines the change of the direction of travel from "mainly to the outlet" to "mainly to the bottom of the clarifier ".

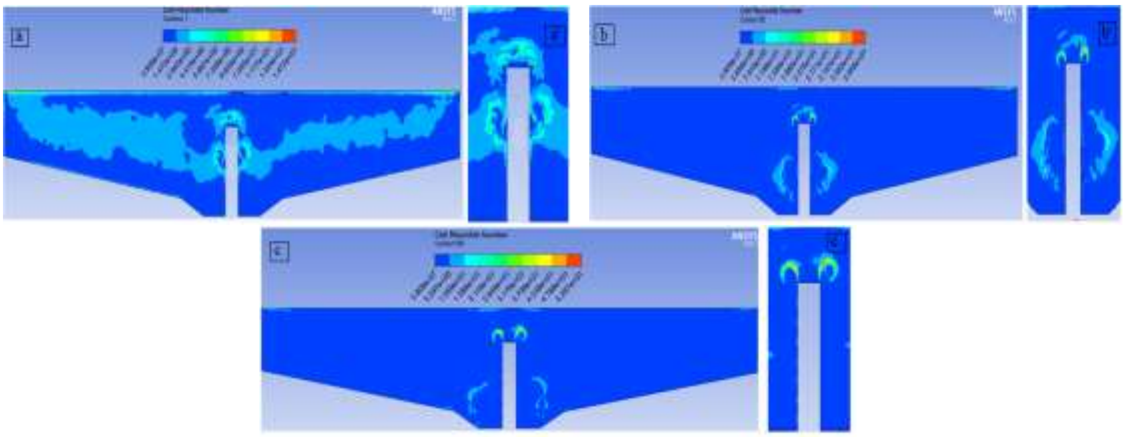

Fig. 5.20. The distribution of the Reynolds number along the length of the geometric model for the clarifier with 1 m feeding pipe at 60 s (a), 120 s (b) and 180 s (c), respectively details of the feeding area, in the same time intervals (a'-c')

c. Turbulence intensity for the clarifier with the feeding pipe of 1 m

In Figure 5.21. is presented the distribution of turbulence intensity along the length of the geometric model for the clarifier with the feeding pipe of 1 m, at 60, 120 and 180 s.

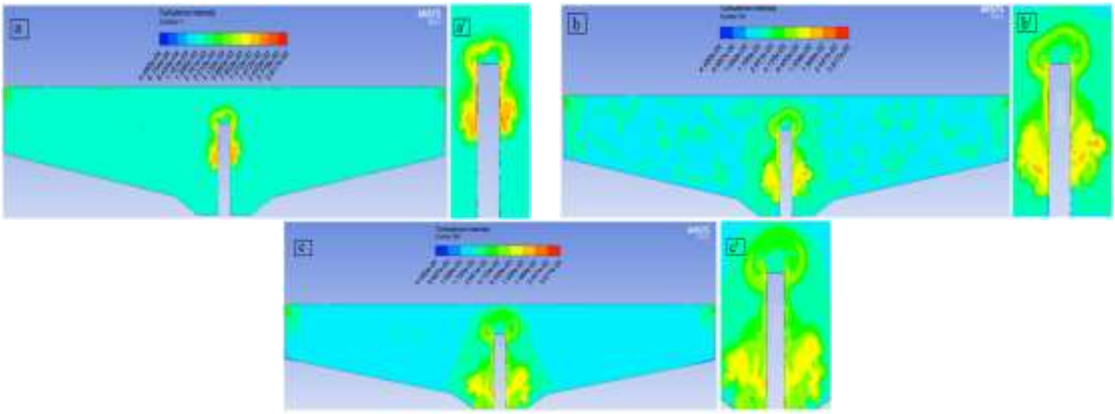

Fig. 5.21. The distribution of the turbulence intensity along the length of the geometric model for the clarifier with 1 m feeding pipe at 60 s (a), 120 s (b) and 180 s (c), respectively details of the feeding area, in the same time intervals (a'-c')

Over time, the areas of maximum turbulence intensity are getting closer and closer to the bottom of the clarifier.

a1) ***Fluid velocity for the clarifier with flared feeding pipe of 2 m***

Figure 5.22 shows the velocity distribution for the clarifier with the feeding pipe of 2 m at 60 s, 120 s and 180 s. It can be seen that, although the velocity in the feeding area has been set to 0.009 m/s, there are areas in the clarifier where the velocity can reach 0.026 m/s. Making a report of the maximum velocities obtained in the clarifier between the two analyzed cases it can be said that the maximum fluid velocity in the case of the clarifier with feeding pipe of 2 m is four times lower than in the case of the clarifier with feeding pipe of 1 m.

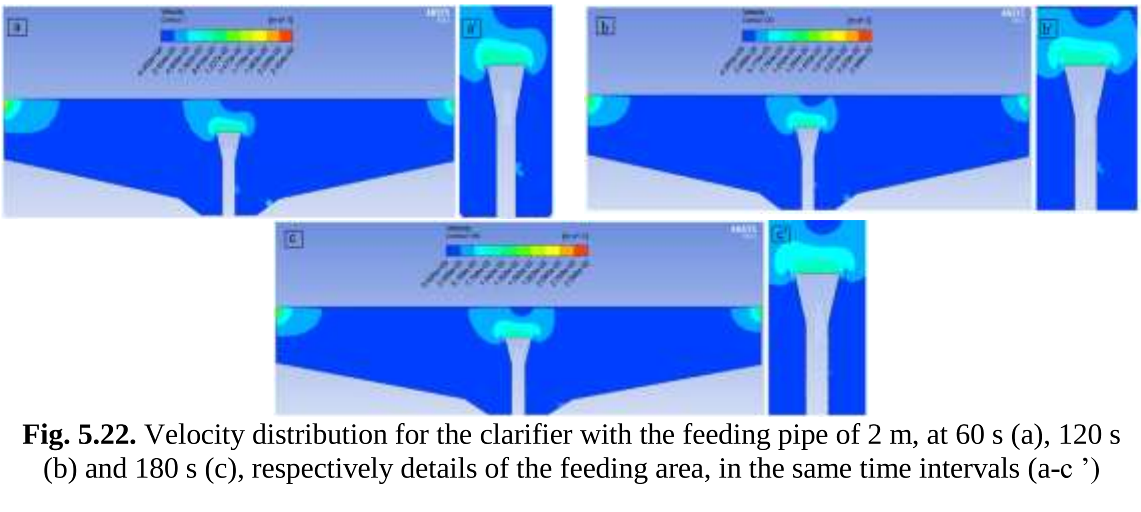

Fig. 5.22. Velocity distribution for the clarifier with the feeding pipe of 2 m, at 60 s (a), 120 s (b) and 180 s (c), respectively details of the feeding area, in the same time intervals (a-c ')

b1) Reynolds number for the clarifier with 2 m feeding pipe

Figure 5.26 shows the distribution of the Reynolds number along the length of the geometric model for the clarifier with the feeding pipe of 2 m, at 60 s, 120 s and 180 s.

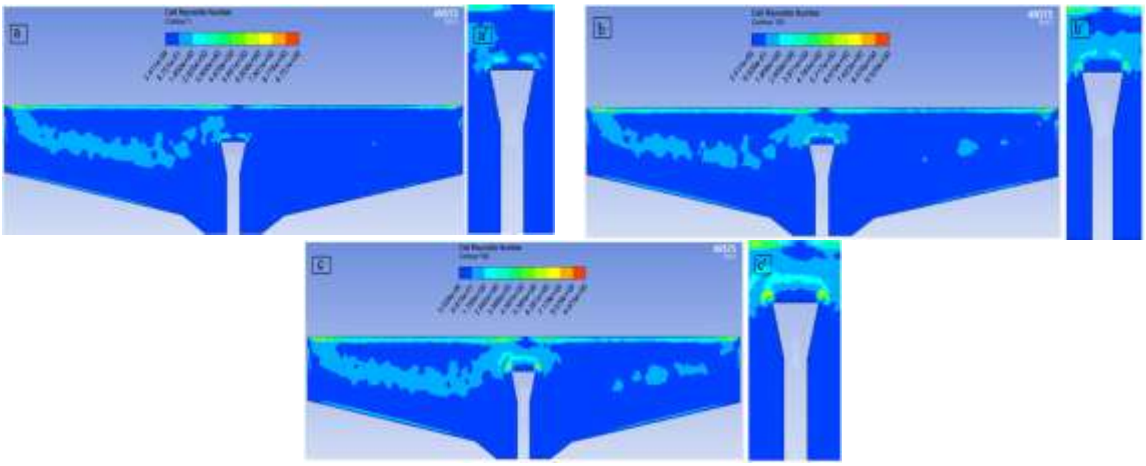

Fig. 5.26. The distribution of the Reynolds number along the length of the geometric model for the clarifier with the feeding pipe of 2 m, at 60 s (a), 120 s (b) and 180 s (c), respectively details of the feeding area, in the same time intervals (a'-c')

Regarding the evolution of the Reynolds number over time, it can be said that its tendency is to decrease, unlike the previously analyzed clarifier which had a tendency to increase the Reynolds number.

c1) Turbulence intensity for the clarifier with the feeding pipe of 2 m

Figure 5.27 shows the distribution of turbulence intensity along the length of the geometric model for the clarifier with the feeding pipe of 2 m, at 60 s, 120 s and 180 s.

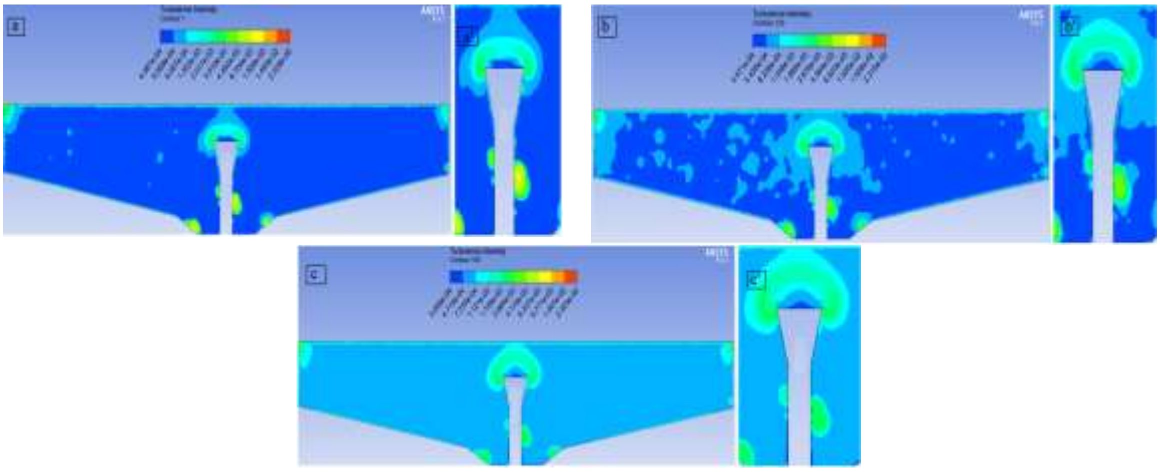

Fig. 5.27. The distribution of the turbulence intensity along the length of the geometric pattern for the clarifier with the feed pipe of 2 m, at 60 s (a), 120 s (b) and 180 s (c), respectively details of the feed area, in the same time intervals (a'-c')

These values of turbulent intensity are also lower than in the first case analyzed.

5.5. Conclusions

In order to anticipate the settling rate of solid particles in wastewater, the theory of dimensional analysis was applied for the mathematical modeling of this process, being considered in the study a number of 7 main parameters that influence the settling process.

Comparing the maximum velocities obtained in the clarifier between the two analyzed cases, it can be said that the maximum fluid velocity in the case of the clarifier with 2 m feeding pipe is four times lower than in the case of the clarifier with 1 m feeding pipe, and the areas of maximum turbulence intensity are in the outlet zones, in the case of the clarifier with a pipe diameter in the feeding zone of 2 m, while, for the clarifier with a pipe diameter of 1 m, the areas of maximum turbulence intensity are closer to the bottom of the clarifier. It is thus recommended to use the clarifier with flared feeding pipe, with a diameter of 2 m in the water feeding area in the clarifier in order to maximize the efficiency of the settling process.

CHAPTER 6. EXPERIMENTAL RESEARCH ON THE WASTEWATER TREATMENT PROCESS BY SETTLING

6.1. Objectives of experimental research

The main objective of the experimental research within this chapter was the influence of the main factors on the settling process, factors that are related to the solid component (size, density and concentration), to the liquid component (density and viscosity), as well as determining the efficiency of radial clarifiers in urban wastewater treatment plants.

The specific objectives of the experimental research were represented by:

- determining the influence of the concentration of suspended solids on the settling in the stationary column;
- determining the turbidity by means of standard samples;
- determining of the variation of the concentration of solid particles in an aqueous suspension with the help of the UV-VIS spectrophotometer;
- determining the clarification curve of an aqueous suspension of solid particles, using the intelligent Raspberry Pi system;
- determining the sedimentation rate of solid particles in the case of three types of suspensions;
- improving the settling process by adding coagulants;
- determining the concentration of solid particles at the inlet and outlet of a clarifier from a treatment plant in January and July;
- recovery of solid waste retained from wastewater by mechanical methods (screening);
- determining the quantity of solid waste retained by the screening facilities, but also of the content of suspended matter of the influent and effluent of a treatment plant.

6.2. Apparatus and equipment used in experimental research

The experiments within this chapter were carried out in the period 2016-2020, in the Depollution Systems Laboratory and in the Microbiology Laboratory, from the Faculty of Biotechnical Systems Engineering, Biotechnical Systems Department, as well as in two urban wastewater treatment plants, from the territory of Romania.

In order to meet the objectives of the experimental research, the steps presented in Fig. 6.1, representing the general methodology of experimental determinations.

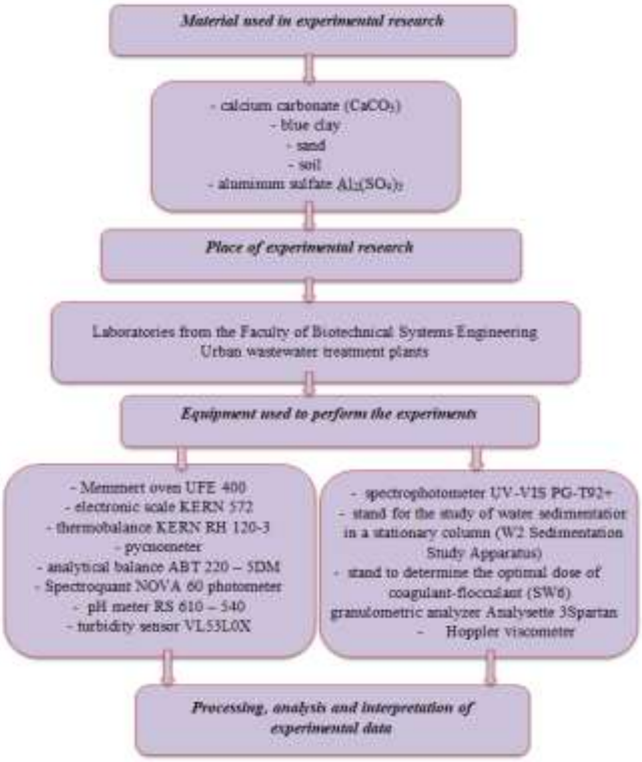

Fig. 6.1. General methodology of experimental determinations

In order to go through all the proposed stages, various equipment and experimental stands were used, the most important of which are: *the experimental stand for the study of sedimentation* (W2-Armfield, UK), is represented by an equipment that allows sedimentation in a stationary column*; experimental stand for the study of coagulation - flocculation* (W1-Armfield, UK), built especially for the analysis of the coagulation process; + *spectrophotometer UV-VIS PG-T92* allows direct recording of the sample and reference signal ratio; *particle size analyzer with sieve Analysette 3 Spartan* (Fritsch), is used to analyze the particle size of solids.

Other equipment used were: Memmert oven UFE 400, thermobalance KERN RH-120-3, analytical balance Kern ABT 220 – 5 DM, electronic scale Kern 572, pH meter RS 610 – 540, Spectroquant NOVA 60 photometer, pycnometer, turbidity sensor VL53L0X and Hoppler viscometer with falling ball.

6.3. Experimental laboratory research on the settling process

6.3.1. Research on the influence of solid particle concentration in the liquid-solid mixture

To analyze the influence of the concentration of solid particles on the settling process, was used the experimental stand W2 - Armfield. All five transparent graded columns with which the stand is provided were used.

In the experiments were analyzed three samples consisting of an aqueous suspension composed of water and blue clay - sample 1 (solid particle size 0.2 mm), water and calcium carbonate ($CaCO_3$) - sample 2 (solid particle size 0.2 mm) and water and soil - sample 3 (solid particle size 0.4 mm).

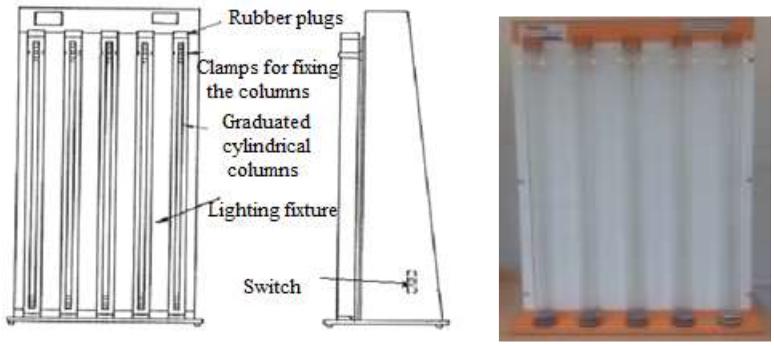

Fig. 6.2. Schematic of the apparatus for the study of settling in stationary column W2 - Armfield, [125]

The experimental study of the settling process in the stationary column of different aqueous suspensions of solid particles has as main result the possibility to obtain clarification curves. In this case, the clarification curves were drawn based on the height of the positions of the clear water-suspension interfaces over time, using the lighting system with which the stand is provided (recordings were carried out over a period of 100 minutes with recordings of the interface positions at 5 min intervals). The experimental results obtained in the sedimentation process in the stationary column, for the three types of suspension, are presented in Table 6.1.

Table 6.1. Experimental results obtained in the settling process for the tree types of suspension regarding the position of the liquid-solid interface

Time, min	Position of the clear water - suspension interface for the tree types of samples analyzed, in the case of the five concentrations, mm														
	Blue clay (0.2 mm)					Calcium carbonate (0.2 mm)					Soil (0.4 mm)				
	2%	4%	6%	8%	10%	2%	4%	6%	8%	10%	2%	4%	6%	8%	10%
0	745	745	745	745	745	745	745	745	745	745	743	748	749	748	747
5	685	692	715	725	729	485	587	689	726	734	614	739	746	747	745
10	635	668	672	684	694	236	477	640	707	720	544	724	704	716	714
15	553	584	630	640	643	113	418	596	690	708	480	576	637	634	697
20	515	538	565	624	618	89	379	570	674	691	295	495	513	485	435
25	449	459	510	515	555	75	356	547	657	683	214	356	363	324	290
30	405	420	490	503	528	70	333	527	640	670	118	192	204	225	214
35	351	394	433	467	494	68	314	511	625	659	43	88	96	117	110
40	272	278	412	426	460	65	295	496	610	647	26	47	59	87	97
45	214	234	348	356	387	64	272	480	595	635	23	40	58	85	96
50	148	177	316	326	318	62	259	466	581	623	22	40	58	84	96
55	115	122	264	291	268	60	244	453	567	613	22	40	58	84	95
60	30	54	217	234	247	59	228	439	555	601	22	40	58	83	95
65	29	53	200	212	232	57	212	426	542	590	22	39	58	83	95
70	29	52	130	168	174	56	198	413	529	578	22	39	58	83	95
75	29	51	115	155	161	55	185	402	519	568	21	38	57	82	95
80	28	51	108	135	157	54	172	388	506	555	21	38	57	82	95
85	28	50	101	129	149	53	163	378	497	547	20	38	57	82	95
90	28	49	98	112	144	52	152	366	486	536	20	38	57	82	94
95	28	49	92	98	137	52	143	354	475	520	20	38	57	82	94
100	28	48	87	95	128	51	135	344	452	516	20	38	57	82	94
after 24h	27	44	82	94	97	49	132	341	400	514	19	37	56	81	93

The experimental data were processed using Microsoft Excel (by applying exponential regression analysis for each concentration, for the three samples analyzed), being graphically represented the variation of the position of the interface clear water - suspension over time. Figure 6.13 shows the time-varying curves of the clear water-suspension interface for blue clay, for all five concentrations.

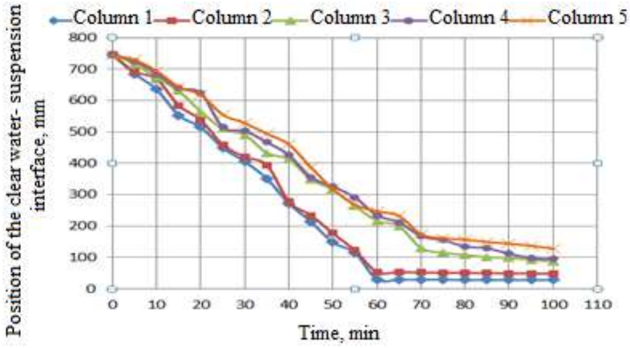

Fig. 6.13. Time-varying curves of the clear water-suspension interface (blue clay)

Mathematically, the relationship between the concentration of solid particles and the zonal settling rate can be described by an exponential regression function, first used in the work [152] eq. (6.1):

$$v = v_0 \cdot e^{-r \cdot X_{TSS}} \tag{6.1}$$

where v_0 – maximum sedimentation rate, (m/s); r – model constant; X_{TSS} – solid particle concentration, (%).

The correlation with the experimental data given by the coefficient R^2, with the coefficients of the regression functions v_0, r and X_{TSS} for sample 1, for the five columns, are presented in Table 6.2.

Table 6.2. The values of the coefficients of the exponential regression function v_0, r and X_{TSS} and the correlation R^2, for sample 1

	Concentration, %	v_0, m/s	r	R^2	X_{TSS}, %	v, m/s
Sample 1	2	1001.6	0.042	0.903	2	$1.534 \cdot 10^{-2}$
	4	909.81	0.034	0.917	4	$1.324 \cdot 10^{-2}$
	6	913.9	0.025	0.971	6	$1.311 \cdot 10^{-2}$
	8	912.01	0.023	0.983	8	$1.265 \cdot 10^{-2}$
	10	872.57	0.02	0.974	10	$1.191 \cdot 10^{-2}$

Figure 6.14 shows the time variation of the position of the clear water - suspension interface for sample 2.

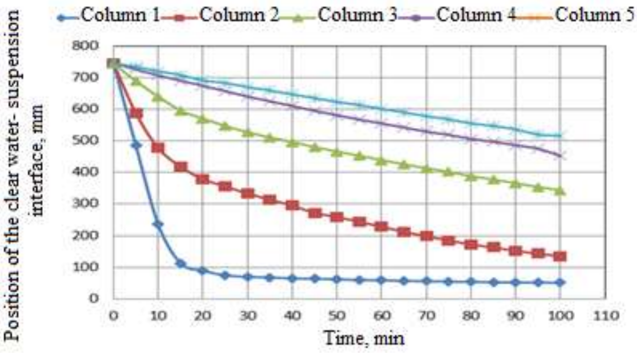

Fig. 6.14. Time-varying curves of the clear water-suspension interface (calcium carbonate)

The distribution of the exponential regression function has the same form as in the case of sample 1 (eq. 6.1), the results obtained in this case being presented in Table 6.3.

Table 6.3. The values of the coefficients of the exponential regression function v_0, r and X_{TSS} and the correlation R^2, for sample 2

	Concentration, %	v_0, m/s	r	R^2	X_{TSS}, %	v, m/s
Sample 2	2	748.47	0.004	0.999	2	$1.238 \cdot 10^{-2}$
	4	741.05	0.005	0.998	4	$1.212 \cdot 10^{-2}$
	6	675.96	0.007	0.978	6	$1.080 \cdot 10^{-2}$
	8	562.97	0.015	0.964	8	$0.832 \cdot 10^{-2}$
	10	207.16	0.018	0.579	10	$0.288 \cdot 10^{-2}$

The graphical representation of the distribution of the position of the clear water - suspension interface for sample 3 is presented in Fig. 6.15.

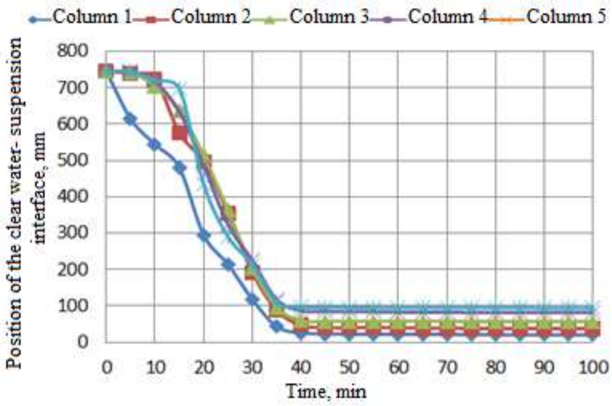

Fig. 6.15. Time-varying curves of the clear water-suspension interface (soil)

The distribution of the exponential regression function has the same shape as in sample 1 and 2 (eq. 6.1), the correlation with the experimental data given by the coefficient R^2, with the coefficients of regression functions v_0 and r for sample 3, for the five columns, are presented in Table 6.4.

Table 6.4. The values of the coefficients of the exponential regression function v_0, r and X_{TSS} and the correlation R^2, for sample 3

	Concentration, %	v_0, m/s	r	R^2	X_{TSS}, %	v, m/s
Sample 3	2	413.76	0.04	0.766	2	$0.637 \cdot 10^{-2}$
	4	549.69	0.035	0.764	8	$0.796 \cdot 10^{-2}$
	6	543.72	0.03	0.737	6	$0.757 \cdot 10^{-2}$
	8	539.42	0.025	0.735	8	$0.736 \cdot 10^{-2}$
	10	521.12	0.023	0.707	10	$0.690 \cdot 10^{-2}$

Following the experiment, we can conclude:

- as lower the concentration of the suspension is, the settling process takes place faster, and as the concentration of particles increases, so does the time required to remove them from wastewater because their sedimentation rate decreases;

- clay and soil require a shorter removal time from wastewater due to density, while for the removal of calcium carbonate, the time required is longer.

6.3.2. Determination of turbidity of the liquid-solid mixture at the height of the settling column, using standard samples

The determinations were performed on the laboratory stand W2 Sedimentation Studies Apparatus (ARMFIELD, UK) equipped with five graduated glass columns, transparent, with an inner diameter of 50 mm and a useful height of 940 mm, which corresponds to a useful volume of 1850 mL. An aqueous suspension of calcium carbonate ($CaCO_3$) particles was used, with concentrations of 2%, 4%, 6%, 8% and 10%, respectively, corresponding to amounts of 37 g, 74 g, 111 g, 148 g and 185 g $CaCO_3$.

The height of the columns was divided into eight zones of 100 mm each, starting from top to bottom, the concentration of solid suspensions in the 8 zones was analyzed by turbidity using standard samples of different concentrations: 0.2 mg/mL, 0.5 mg/mL, 1 mg/mL, 2 mg/mL, 4 mg/mL and 6 mg/mL, specially prepared for this purpose in bottles of 100 mL. In fact, it was analyzed how the concentration of the suspension decreases in each of the 8 areas, at intervals of 5 min, for a time of determinations of 100 min.

Table 6.5 shows the distribution of solid particle concentration over time, for the 2% concentration column, analyzing all 8 established zones.

Table 6.5. Experimental data of turbidity in the 8 zones for the column with the concentration of suspension 2%

Time, min	Concentration of zones, mg/mL							
	1	2	3	4	5	6	7	8
0								
5	6							
10	4	6						
15	2	4	6					
20	2	2	4	6				
25	1	2	4	6				
30	1	2	2	4	6			
35	1	2	2	2	4	6		
40	1	2	2	2	4	6		
45	1	2	2	2	2	4	6	
50	1	1	2	2	2	4	4	6
55	1	1	2	2	2	2	4	4
60	0.5	1	1	2	2	2	2	4
65	0.5	1	1	1	1	1	1	2
70	0.5	0.5	1	1	1	1	1	1
75	0.5	0.5	1	1	1	1	1	1
80	0.5	0.5	1	1	1	1	1	1
85	0.5	0.5	0.5	1	1	1	1	1
90	0.5	0.5	0.5	1	1	1	1	1
95	0.5	0.5	0.5	1	1	1	1	1
100	0.5	0.5	0.5	1	1	1	1	1

For the graphical analysis of the zones in the 2% $CaCO_3$ concentration column, a power-type regression function was applied, function applied for all five concentrations. Therefore, the decrease of turbidity, in fact the concentration of the suspension in each analyzed zones follows a power distribution of the form:

$$Tb = a \cdot t^{-b} \qquad (6.2)$$

where t is the time, (s); a and b are the process parameters, determined experimentally.

Table 6.6. The values of the coefficients of the power regression function a, b and of the correlation coefficient R^2

Turbidity, zones		a	b	R^2
$C_{2\%}$	1	24.008	0.875	0.936
	2	87.203	1.13	0.905
	3	222.82	1.294	0.905
	4	226.24	1.223	0.895
	5	979.49	1.556	0.887
	6	8936	2.052	0.869
	7	31902	2.335	0.771
	8	234137	2.768	0.796

Figure 6.17a shows the correlation between the turbidity related to the analyzed zones and the turbidity change time, but also the value of the zonal concentration after 25 min. (Fig. 6.17b). It should be noted that the value of the initial concentration of solid particles in the

column was 20 mg/mL, the decrease being considerable. The last zone that reaches a turbidity of 0.5 mg/mL was zone 3. Analyzing the graphs corresponding to each sedimentation zone, it can be seen that the value of the correlation coefficient has a decreasing variation from sedimentation zone 1 to zone 8.

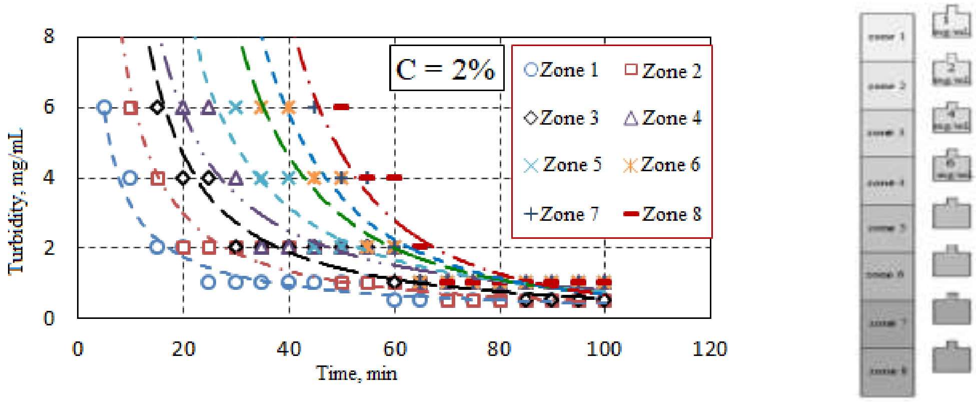

a b

Fig. 6.17. The variation of turbidity in time, for the 8 analyzed zones, for the concentration column 2% (a) and the turbidity value for the analyzed zones in min. 25 (b)

Table 6.7 shows the data obtained for the 4% concentration column. In this case, too, the same steps were taken as in the case of the 2% concentration column.

Table 6.7. Experimental data of turbidity in the 8 zones for the column with the concentration of suspension 4%

Time, min	Concentration of zones, mg/mL							
	1	2	3	4	5	6	7	8
0								
5	6							
10	6	6						
15	4	6						
20	4	4	6					
25	2	4	4	6				
30	2	4	4	4	6			
35	2	2	4	4	4	6		
40	2	2	2	4	4	6		
45	2	2	2	2	4	4	6	
50	2	2	2	2	4	4	6	
55	1	2	2	2	2	4	6	
60	1	2	2	2	2	4	4	6
65	1	1	2	2	2	2	2	4
70	1	1	1	1	2	2	2	4
75	1	1	1	1	1	1	2	2
80	1	1	1	1	1	1	1	2
85	1	1	1	1	1	1	1	2
90	0.5	1	1	1	1	1	1	1
95	0.5	1	1	1	1	1	1	1
100	0.5	0.5	1	1	1	1	1	1

Analyzing Table 6.6 in which the experimental data are presented, it can be seen that only the first two zones of the column reached the value of the concentration of solid particles of 0.5 mg/mL $CaCO_3$ in the 100 min.

The distribution of the power regression function has the same shape as in the case of the 2% concentration column, the results being presented in Table 6.6. It is noted that the second column analyzed had an initial suspension concentration of 40 mg/mL.

Table 6.6. The values of the coefficients of the power regression function a, b and of the correlation coefficient R^2

Turbidity, zones		a	b	R^2
$C_{2\%}$	1	24.008	0.875	0.936
	2	87.203	1.13	0.905
	3	222.82	1.294	0.905
	4	226.24	1.223	0.895
	5	979.49	1.556	0.887
	6	8936	2.052	0.869
	7	31902	2.335	0.771
	8	234137	2.768	0.796

From the analysis of the graph (Fig. 6.18) it can be seen that the turbidity in each area decreases over time, the sedimentation zone 8 showed a correlation coefficient R^2 = 0.933.

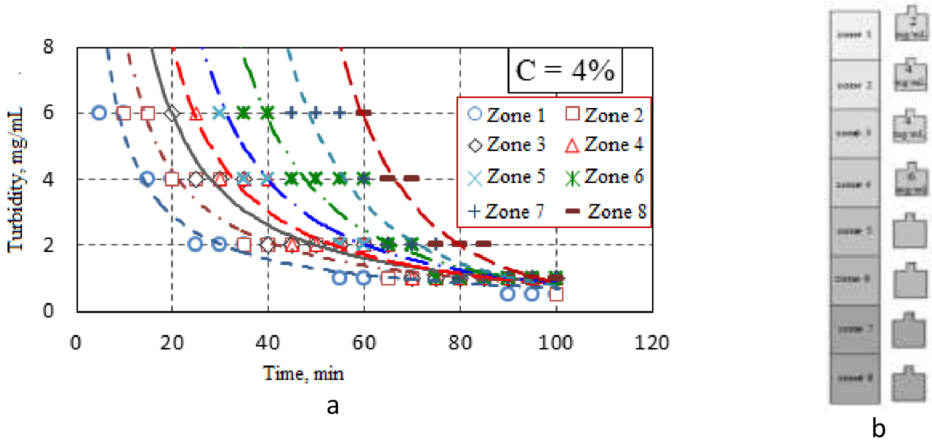

Fig. 6.18. The variation of turbidity in time, for the 8 analyzed zones, for the concentration column 4% (a) and the turbidity value for the analyzed zones in min. 25 (b)

The distribution of the concentration of solid particles on zones in the sedimentation column of 6% concentration is presented in Table 6.9 and in Fig. 6.19. In this case were followed the same steps as in the previous cases.

Table 6.9. Experimental data of turbidity in the 8 zones for the column with the concentration of suspension 6%

Time, min	Concentration of zones, mg/mL							
	1	2	3	4	5	6	7	8
0								
5								
10	6							
15	4	6						
20	4	4	6					
25	4	4	6					
30	4	4	4	6				
35	4	4	4	6				
40	4	4	4	4	6			
45	2	4	4	4	6			
50	2	2	4	4	4	6		
55	2	2	2	4	4	6		
60	2	2	2	2	4	4	6	
65	2	2	2	2	4	4	6	
70	1	2	2	2	2	4	6	6
75	1	1	2	2	2	4	4	6
80	1	1	1	2	2	2	4	4
85	1	1	1	2	2	2	2	4
90	1	1	1	1	1	1	2	2
95	1	1	1	1	1	1	1	2
100	1	1	1	1	1	1	1	1

For all eight sedimentation zones, the power type function was used in the analysis of the experimental data. It can be seen that none of the zones has not reached the level of clarity of 0.5 mg/mL suspension of $CaCO_3$. More than that, it is observed that in the sedimentation zone 8 only after minute 70 the concentration of solid particles decreases to 6 mg / mL.

Table 6.10. The values of the coefficients of the power regression function a, b and of the correlation coefficient R^2

Turbidity, zones		a	b	R^2
$C_{6\%}$	1	62.585	0.892	0.837
	2	128.24	1.045	0.846
	3	363.33	1.27	0.879
	4	1328.1	1.533	0.889
	5	18002	2.11	0.896
	6	657470	2.897	0.872
	7	1E+08	3.971	0.884
	8	9E+09	4.914	0.896

In the fourth column, in which the concentration of the suspension was 8% $CaCO_3$, the initial turbidity of the solid particles was 111 mg/mL. Proceeding as in the previous cases, the experimental data presented in Table 6.11 were obtained.

The content of solid particles is quite high, which causes an increase in the clarification time, so it was possible to check the concentration of 6 mg/mL in the sedimentation zone 8 only in minute 100.

Table 6.11. Experimental data of turbidity in the 8 zones for the column with the concentration of suspension 8%

Time, min	Concentration of zones, mg/mL							
	1	2	3	4	5	6	7	8
0								
5								
10								
15	6							
20	6	6						
25	6	6						
30	4	6	6					
35	4	4	6					
40	4	4	6					
45	4	4	4	6				
50	4	4	4	6				
55	4	4	4	4	6			
60	2	4	4	4	6			
65	2	2	4	4	6			
70	2	2	4	4	6	6		
75	2	2	4	4	4	6		
80	2	2	2	4	4	6	6	
85	2	2	2	4	4	4	6	
90	1	2	2	2	4	4	6	
95	1	2	2	2	2	4	4	
100	1	1	2	2	2	2	4	6

It can be noticed, according to the recorded data, that six of the eight zones do not reach the concentration of 1 mg / mL after the 100 min test (sedimentation zone 3, zone 4, zone 5, zone 6, zone 7 and zone 8). More than that, in sedimentation zone 6, the concentration level of 2 mg / mL is barely reached in minute 100.

Table 6.12. The values of the coefficients of the power regression function a, b and of the correlation coefficient R^2

Turbidity, zones		a	b	R^2
$C_{8\%}$	1	98.093	0.906	0.811
	2	140.31	0.965	0.819
	3	230.03	1.022	0.806
	4	812.42	1.274	0.734
	5	2150	1.43	0.701
	6	583487	2.664	0.749
	7	83698	2.158	0.735
	8	-	-	-

The graphical representation of the experimental data (Fig. 6.20) was made, also in this case, by using the power type function.

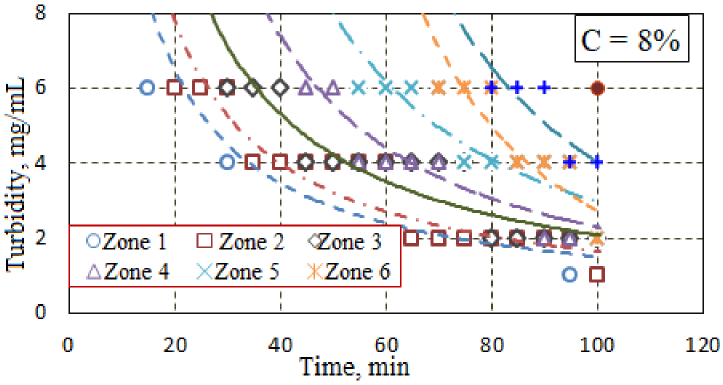

a

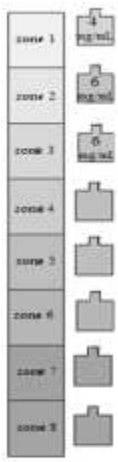

b

Fig. 6.20. The variation of turbidity in time, for the 8 analyzed zones, for the concentration column 8% (a) and the turbidity value for the analyzed zones in min. 25 (b)

The last column analyzed in terms of solid particle concentration, analogous to the other four previous concentrations, was the 10% concentration. The experimental results obtained are presented in Table 6.13.

In this column, the initial turbidity value was 100 mg / mL, a fairly high value compared to the highest value of the standard samples, namely 6 mg / mL.

In the first sedimentation zone, the solid particle concentration level of 6 mg/mL was reached after 15th minute after the start of the experiment, and the concentration of 4 mg/mL, also for this zone, was reached after 45 min.

Table 6.13. Experimental data of turbidity in the 8 zones for the column with the concentration of suspension 10%

Time, min	Concentration of zones, mg/mL							
	1	2	3	4	5	6	7	8
0								
5								
10								
15	6							
20	6							
25	6							
30	6	6						
35	6	6						
40	6	6						
45	4	6						
50	4	6	6					
55	4	6	6					
60	4	4	6					
65	4	4	4	6				
70	2	4	4	4	6			
75	2	4	4	4	6			
80	2	2	4	4	6			
85	2	2	2	4	4	6		
90	2	2	2	2	4	6		
95	1	2	2	2	4	6		
100	1	2	2	2	2	4	6	

It can be noticed that only in sedimentation zone 1 the concentration of 1 mg/mL is reached in minute 95, this being the lowest concentration of the suspension recorded in the 100 min.

More than that, it can be observed that in sedimentation zone 7, the appearance of this concentration takes place only at minute 100, fact for which, for zone 7 and 8 it was not possible to represent graphs of variation of turbidity in time, the last represented zone being the sedimentation zone 6.

Table 6.14. The values of the coefficients of the power regression function a, b and of the correlation coefficient R^2

Turbidity, zones		a	b	R^2
$C_{10\%}$	1	127.69	0.937	0.729
	2	418.25	1.147	0.784
	3	9470.6	1.342	0.806
	4	41721	2.129	0.715
	5	544215	2.635	0.676
	6	116579	2.204	0.578
	7	-	-	-
	8	-	-	-

The experiment presented shows that the zonal variation of the suspension clarity can be represented by a law of variation of power type (or exponential type), and the parameters of the equation depend on the initial concentration of the suspension, without taking into account the particle size distribution of the solid particles or the temperature at which the settling process takes place.

6.3.3. Research on the influence of particle size and concentration of aqueous suspension using the UV-VIS Spectrophotometer

The objective of the experiment was to record the variation of the concentration of solid particles, of different sizes, from an aqueous suspension represented by the variation of the absorbance over time.

The experimental research was carried out using an aqueous suspension of distilled water and soil particles - sample 1, water and sand particles - sample 2 and sample 3 - water and calcium carbonate particles, having predetermined concentrations of 0.2%, 0.4%, 0.5%, 1%, 2%, 2.5% and 3%. For all three samples, were analyzed fractions with the particle size between 0 - 0.18 mm, 0.25 - 0.315 mm and 0.5 - 0.7 mm.

For the graphical representation of the experimental data, the Kinetics mode was used - for all three samples (which is part of the spectrophotometer software), which allows kinetic determinations for a single cuvette, with tracing the reaction curve.

Data recording was performed in the absorbance range 0-10 (maximum recording value), for 600 s, with recordings every 5 s, at a wavelength of 600 nm.

Thus, for the beginning is represented the concentration of solid particles by the variation of the absorbance in time for the soil particles with dimensions between 0 - 0.18 mm. In Fig. 6.23 is the correlation between the time of change of the absorbance of the analyzed sample and the value of the absorbance at that moment.

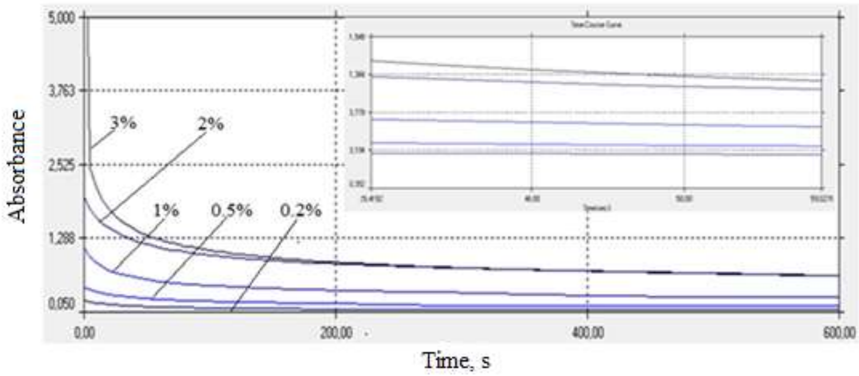

Fig. 6.23. Variation of absorbance over time depending on the concentration of solid particles of soil for concentration values of 3%, 2%, 1%, 0.5% and 0.2%

Analyzing the graph that represents the experimental data, it can observed that the 3% concentration sample and the particle size between 0-0.18 mm reached an absorbance value of 2.483 in 5 s, reaching in the second 600 a value of 0.658. Based on the experimental data recorded by the spectrophotometer and exported to the M. Excel program, the absorbance variations were represented as a function of concentration, variation recorded at 100 s, 200 s and 300 s (Fig. 6.24).

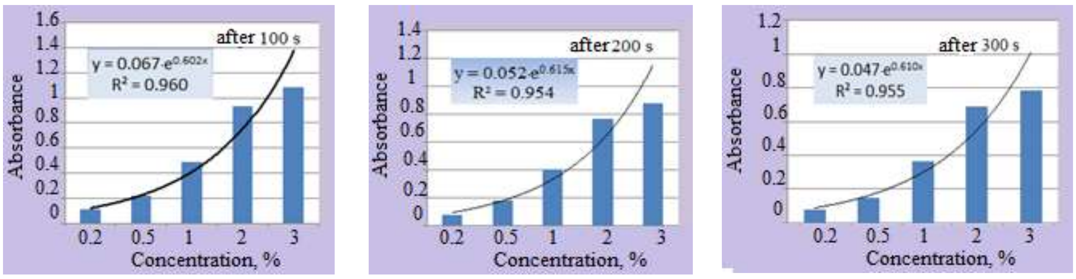

Fig. 6.24. Graphical representation of absorbance as a function of concentration of soil solid particles, at 100 s, 200 s and 300 s

For the graphical analysis was applied an exponential function (also used in sample 2 and 3). For a concentration of 3% of the liquid-solid suspension with dimensions between 0-0.18 mm, the absorbance decreased from 1.08 after 100 s of settling in the spectrophotometer cuvette, to about 0.787 after 300 s of settling of the solid particles .

For the fraction with particle sizes between 0.25-0.315 mm, the experimental data are represented in Fig. 6.25.

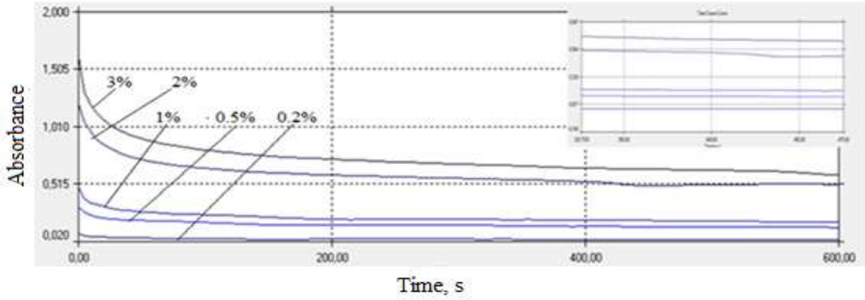

Fig. 6.25. Variation of absorbance over time depending on the concentration of solid particles of soil for concentration values of 3%, 2%, 1%, 0.5% and 0.2%

Thus, similar to the first sample, the variation of the concentration of solid particles, expressed by absorbance, over time was plotted (Fig. 6.26). In this case, the absorbance value for the 3% concentration sample and the particle size between 0.25-0.315 mm decreased from 1.624 in 5 s to 0.593. In the case of the 0,2% concentration sample, the initial absorbance value was 0.068 after 5 s of measurements, reaching 0.034 at the end of measurements.

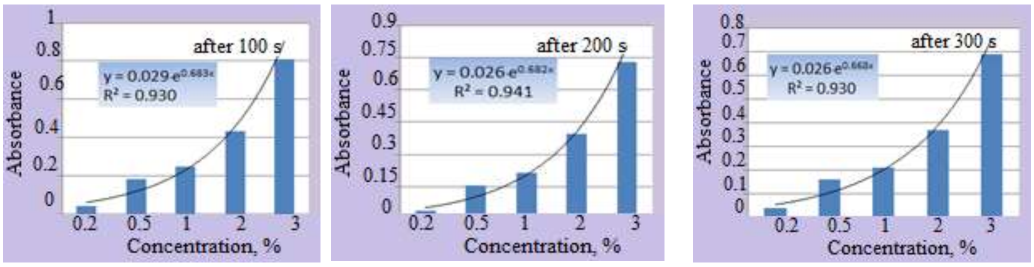

Fig.6.26. Graphical representation of absorbance as a function of concentration of soil solid particles, at 100 s, 200 s and 300 s

Figure 6.27 shows the distribution of the concentration of solid particles with dimensions between 0.5 and 0.7 mm. It is noted that the value reached after 5 s from the start of the recordings, for the concentration of 3% was 1,213 and reached at the end of the measurements a value of 0.618.

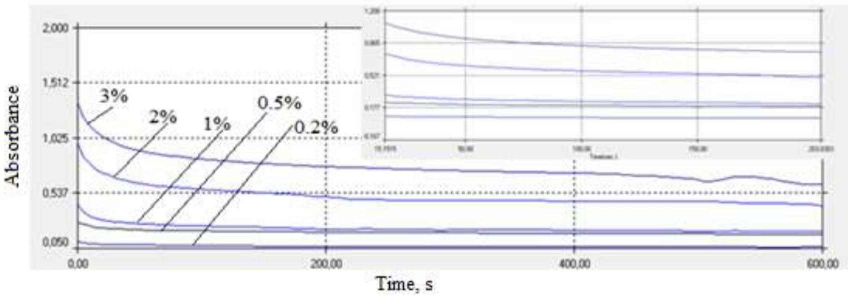

Fig. 6.27. Variation of absorbance over time depending on the concentration of solid particles of soil for concentration values of 3%, 2%, 1%, 0.5% and 0.2%

In the graphs representing the variation of absorbance depending on the concentration of solid particles in Fig. 6.28, recorded at 100 s, 200 s and 300 s, the close correlation between the analyzed parameters was observed, reflected in the high value of the correlation coefficient R^2 (> 0.950).

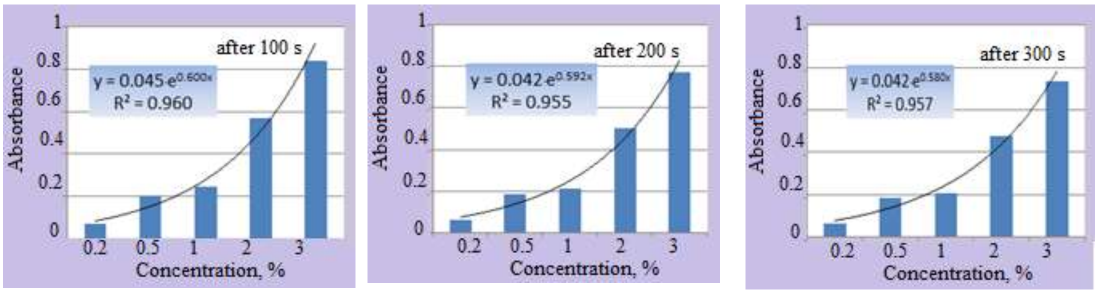

Fig. 6.28. Graphical representation of absorbance as a function of concentration of soil solid particles, at 100 s, 200 s and 300 s

In case of sample 2, the same particle size was analyzed as in sample 1. Thus, in the case of the first fraction with the particle size between 0-0.18 mm, according to Fig. 6.29, for a concentration of 3% of the liquid-solid suspension and particles with the size between 0-0.18 mm, the absorbance decreased by to 1.263 at 0.3 after the solid particle settling process has been completed.

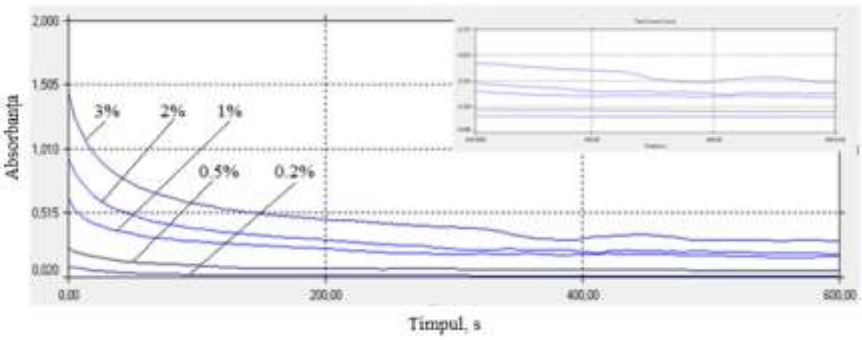

Fig. 6.29. Variation of absorbance over time depending on the concentration of solid particles of sand for concentration values of 3%, 2%, 1%, 0.5% and 0.2%

Making a comparison between sample 1 and sample 2, in terms of particle size, it was observed that the time required to settle the sand particles was much shorter than that of the soil, the absorbances having values about twice lower at the initial time and about ten times smaller at the end of the recordings.

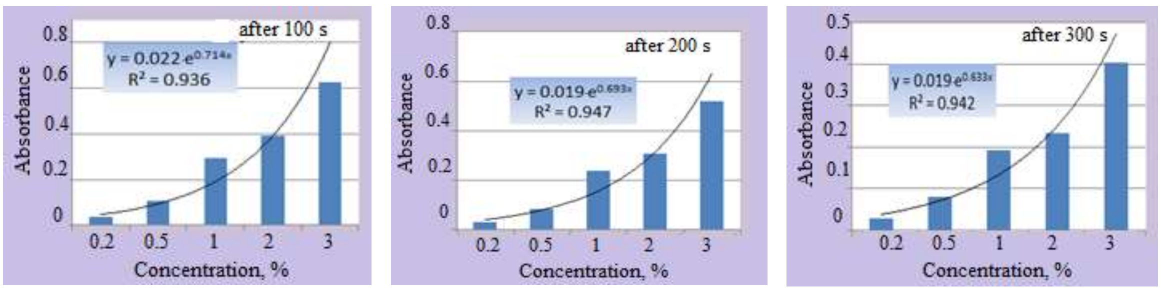

Fig. 6.30. Graphical representation of absorbance as a function of concentration of sand solid particles, at 100 s, 200 s and 300 s

For particles with dimensions between 0.25 - 0.315 mm, the experimental data on absorbance are represented in Fig. 6.31. In this case, only two samples related to the concentration of 3 and 2.5% were analyzed. This was due to the fact that the absorbance value decreased very slowly, starting from a rather low absorbance value.

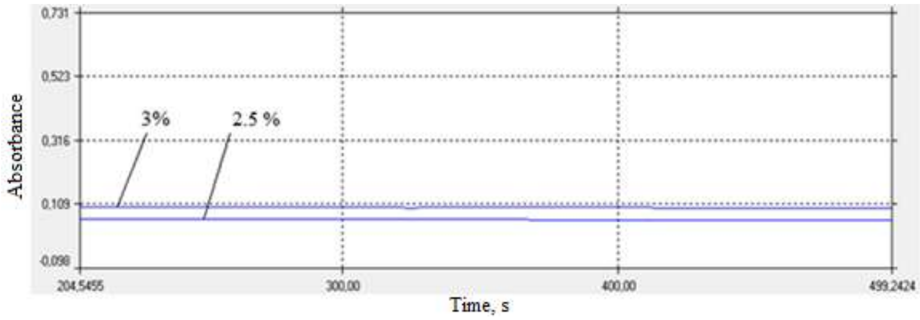

Fig. 6.31. Variation of absorbance over time depending on the concentration of solid particles of sand for concentration values of 3% and 2.5%

Similar to the sand sample with particle sizes between 0.25-0.315 mm analyzed previously, it was proceeded with particle sizes between 0.5-0.7 mm. The initial absorbance value for the 3% concentration was 0.06 and 0.022 for the 0.2% concentration, respectively, and the final value was 0.052 for the 3% concentration and 0.020 for the 0.2% concentration. (Fig. 6.32).

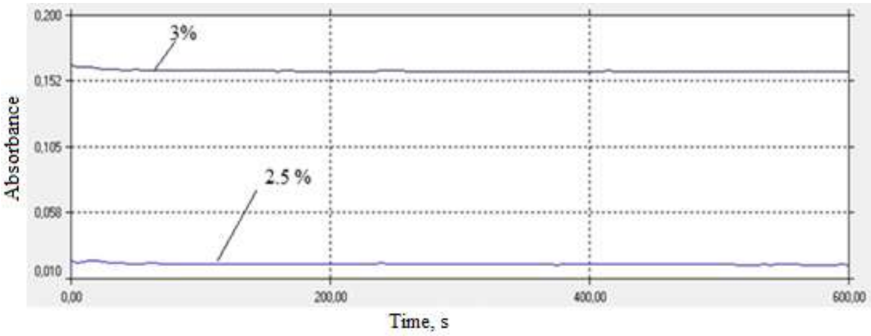

Fig. 6.32. Variation of absorbance over time depending on the concentration of solid particles of sand for concentration values of 3% and 2.5%

For particles with dimensions between 0.25-0.315 mm and 0.5-0.7 mm, respectively, the variation of absorbance as a function of concentration for the three time moments was not represented, the variation being approximately linear. This is due to the high density of sand particles.

In the case of sample 3 with particle sizes between 0-0.18 mm, the graphical representation of the experimental data is present in Fig. 6.33.

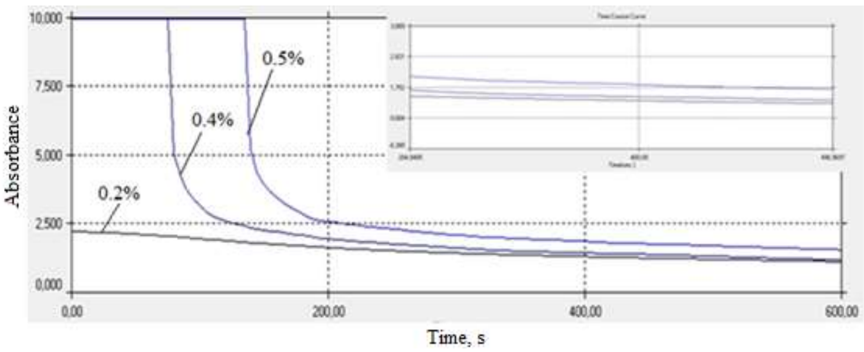

Fig. 6.33. Variation of absorbance over time depending on the concentration of solid particles of calcium carbonate for concentration values of 0.2%, 0.4% and 0.5%

According to Figure 6.33, it is found that unlike sand, where only two of the highest concentrations could be analyzed, in the case of calcium carbonate, due to the lower particle density, it was possible to analyze three concentration values, 0.2%, 0.4% and 0.5%. This is due to the high turbidity at concentrations higher than 0.5%, the absorbance value in this case being higher than 10, it is not possible to record with the spectrophotometer.

Figure 6.34 shows graphically the experimental data for particles with size between 0.25-0.315 mm, the analyzed concentrations being the same from the previous test. Thus, for the concentration of 0.5%, the data could be recorded from 185 seconds, for the concentration of 0.4% from the second 100, and for the concentration 0.2% from the beginning of the measurements.

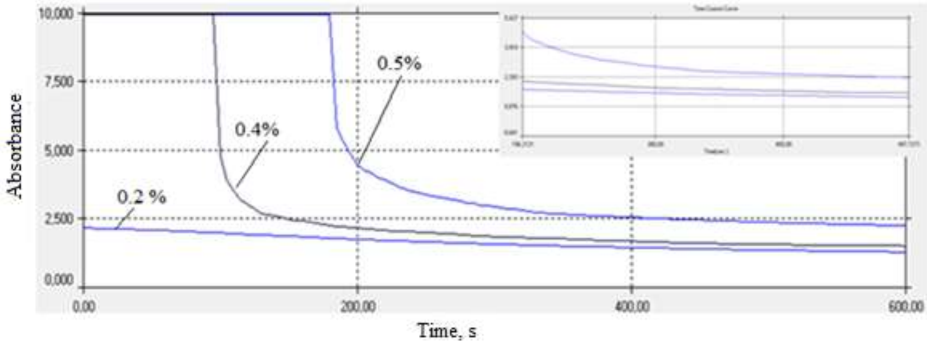

Fig. 6.34. Variation of absorbance over time depending on the concentration of solid particles of calcium carbonate for concentration values of 0.2%, 0.4% and 0.5%

The values obtained for the third fraction with particles of dimensions between 0.5-0.7 mm are presented in Fig. 6.35. Data recording at the 0.5% concentration was possible from the 250 second, for the 0.4% concentration from the 210 second, and for the 0.2% concentration this was possible from the beginning of the measurements.

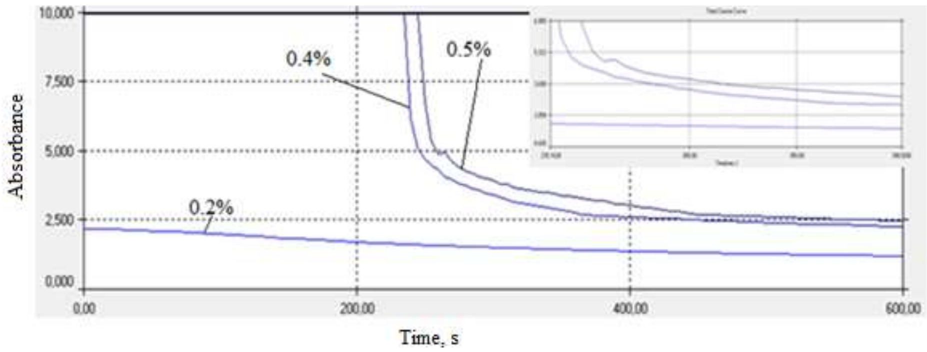

Fig. 6.35. Variation of absorbance over time depending on the concentration of solid particles of calcium carbonate for concentration values of 0.2%, 0.4% and 0.5%

6.3.4. Determination of the clarification curve of an aqueous suspension of solid particles, using the intelligent Raspberry Pi system

Experimental research was carried out in a stationary field on a laboratory stand, consisting on a plexiglass column, with the dimensions: 220 mm long, 30 mm diameter, 100 ml capacity, VL53L0X turbidity sensor, Raspberry Pi device and Pi camera. Recording of the interface between the clarified water area and the sludge area was viewed in real-time on a

PC screen by taking photos at a certain time using a camera connected to the Raspberry Pi device, [164].

The purpose of the experimental research it was to determine the turbidity of the wastewater, the solid particle concentration (TSS) and the settling velocity of the solid particles in the wastewater.

In the following are presented the steps to determine these parameters.

a) regarding the turbidity of the wastewater, it was measure it in three points at different heights on the graduated column, namely at 55 mm, 65 mm and 75 mm respectively. For each set height, the turbidity of the water was measured for about 80 minutes, the measurements being made in increments of 20 seconds.

The measurements were made using a VL53L0X turbidity sensor, and the values recorded in the NTU were converted to mass concentration using the equation, [130]:

$$ln(TSS) = 1.5\, ln(NTU) + 0.15 \quad (6.3)$$

b) regarding the settling velocity of the solid particles, it was determined by calculation using the image processing method of the separation interface between the clarified area and the sludge area with the Pi camera attached to the Raspberry Pi device.

In this study, it was used the mathematical expression proposed by Cho et al. (1993), which introduced the concept of "solid flux" for the calculation of settling. Until now, two empirical models have been successfully used to design clarifiers for solid material flows. These include the power law model (eq. (6.4)) and the exponential model (eq. (6.5)):

$$v = v_0 h^{-n} \quad (6.4)$$

$$v = v_0\, exp(-nh) \quad (6.5)$$

where v_0 – the maximum settling rate, (m/s); h - interface level, (m); n – model constant

In Table 6.15 are data presented for five moments of time:

- the turbidity values determined experimentally at three heights: 75 mm (T_ex75), 65 mm (T_ex65) and 55 mm (T_ex55);
- the turbidity values determined by the regression function: 75 mm, (T_75), 65 mm (T_65) and 55 mm (T_55);
- the mass concentration determined after conversion: 75 mm (Ln TSS_75), 65 mm (Ln TSS_65) și 55 mm (Ln TSS_55).

Table 6.15. Experimental results obtained in the settling process, [164]

Time, s	T_ex75	T_ex65	T_ex55	T_75	T_65	T_55	Ln TSS_75	Ln TSS_65	Ln TSS_55
20	260.009	222.342	246.311	270.452	240.593	285.07	8.491	8.256	8.409
40	277.623	208.035	206.178	194.446	161.506	194.641	8.589	8.156	8.143
60	296.178	237.412	187.623	160.317	127.92	155.702	8.686	8.354	8.001
80	260.009	194.454	183.287	139.801	108.417	132.897	8.491	8.055	7.966
100	277.623	194.454	187.623	125.713	95.362	117.535	8.5893	8.055	8.001

Based on experimental data was plotted the clarification curve corresponding to the three points in which was measured the turbidity. This is shown in Fig. 6.37.

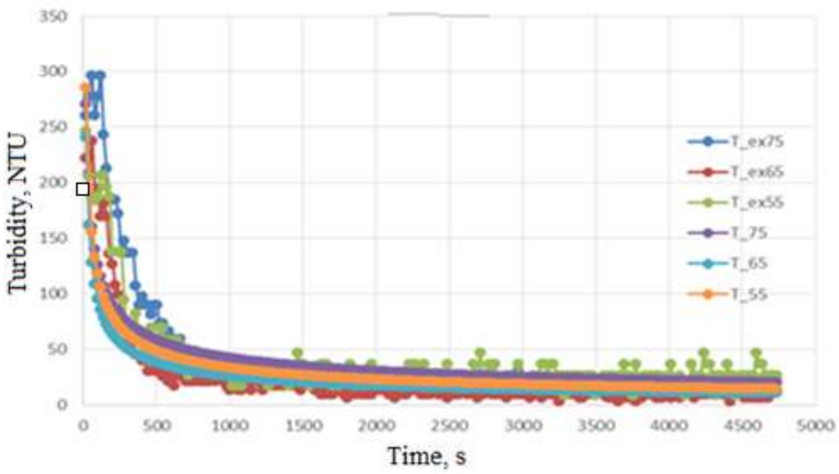

Fig. 6.37. Variation of turbidity in the three measured points, [164]

According to Fig. 6.37, it can be seen that the turbidity value in the 80 minutes in which the measurements were made, for the height of 75 mm decreased from 260 NTU to approx. 11 NTU, for the height of 65 mm the turbidity had values between 222 and 13 NTU, and for the height of 55 mm, the turbidity had variations from 246 to 26 NTU.

Figure 6.39 shows the evolution of sedimentation rate over time, determined by calculation using equation (6.5), following the experimental determination of the level of the separation interface between the clear area and the sludge area, by processing the images captured by means of the Pi camera. In this figure, the magenta colour curve represents the experimentally determined the settling velocity values and with the blue line, the sedimentation velocity values calculated by numerical integration of the differential equation from the model proposed by Je and Chang in their paper[63].

The dotted line in the graphical representation indicates the values of settling velocity calculated analytically by solving the differential equation mentioned above.

It is noticed that at the initial moment, the settling velocity value is 4.5 mm s^{-1}, and in second 120 it decreases to 0.8 mm s^{-1}. Thus it can be concluded that as the time passes, the settling velocity of the solid particles in a suspension decreases.

Figure 6.40 graphically represents the evolution in height of the liquid-solid interface during the experiment. The blue curve represents the variation of the height of the interface between the clarified area and the sludge area determined experimentally, and in red is represented the height of the interface calculated by numerical integration. The green line indicates the height values of the analytically calculated interface by solving the differential equation mentioned above. According to Fig. 6.40, it is observed that the height of the solid particle layer increases over time, inversely proportional to the sedimentation rate.

The experimental results obtained are in correlation with those obtained by Sithebe et al. (2014), as well as those obtained by Je and Chang (2004), [63,130].

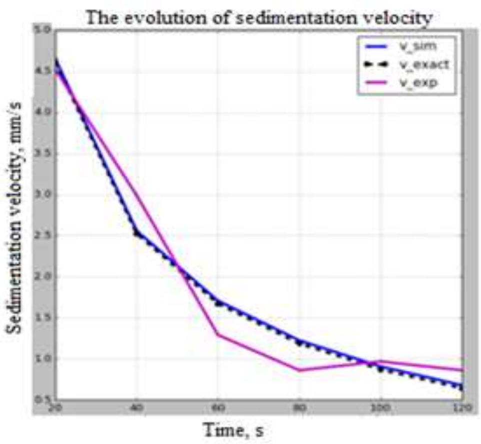

Fig. 6.39. The rate of settling variation over time, [164]

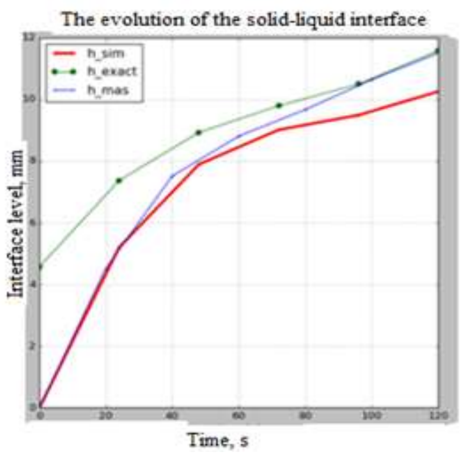

Fig. 6.40. The evolution of the solid-liquid interface, [164]

6.3.5. Determination of settling rate for three types of liquid-solid mixtures

The experiment aimed to determine the settling rate of three types of suspension consisting of water - calcium carbonate, water - soil, water - blue clay, concentrations 2%, 4%, 6%, 8% and 10%. The particle size for calcium carbonate and blue clay was 0.2 mm and that of the soil was 0.4 mm..

To determine the settling rate of the solid particles may be applied to Stokes' law, which has the form (see subchapter 4.1):

$$v = \frac{d_p^2 \cdot g \cdot (\rho_p - \rho_S)}{18 \cdot \vartheta \cdot \rho_S} = \frac{d_p^2 \cdot g \cdot (\rho_p - \rho_S)}{18 \cdot \eta} \tag{6.8}$$

where d_p – particle diameter, (m); g – gravitational acceleration, which has a constant value of 9.81, (m/s^2); ρ_p – solid particle density, (kg/m^3); ρ_s – suspension density, (kg/m^3); η – dynamic viscosity of the suspension, (Pa·s); ϑ –kinematic viscosity of the suspension, (m^2/s).

In order to determine the settling rate, the following parameters were determined: the density of the three types of materials; dynamic density and viscosity of the suspension.

The density of the three types of solid particles was determined using the pycnometer, using the relationship:

$$\rho_p = \frac{(m_c - m_a) \cdot \rho_l}{(m_b + m_c) - (m_a + m_d)} \tag{6.9}$$

where ρ_p represents the density of the analyzed material, (g/cm^3); m_a – empty pycnometer mass (including cap with capillary tube), (g); m_b – the mass of the pycnometer filled with the reference liquid, (g); m_c – mass of the pycnometer with 2-5 g of material, (g); m_d – mass of the pycnometer with material and filled with the reference liquid to the mark, (g); ρ_l – density of the reference liquid, (g/cm^3).

The same steps were performed for all three types of solid particles. For each material, three types of tests were performed, the final density value being the average of the three determinations (ρ_{pm}). Table 6.16 presents the experimental results, which have values close to those found in the literature (ρ_{lit}).

Table 6.16. The experimental results obtained for the calculation of the density for three samples of material, using the pycnometer

Type of material	m_a, g	m_c, g	m_b, g	m_d, g	ρ_l, g/cm^3	ρ_p, g/cm^3	ρ_{pm}, g/cm^3	ρ_{lit}, g/cm^3
Calcium carbonate	25.194	27.315	45.759	47.049	0.86	2.195	2.412	2.93, [173]
	25.196	28.517	45.746	47.941	0.86	2.536		
	25.204	27.975	45.752	47.572	0.86	2.506		
Blue clay	25.284	28.452	45.811	47.733	0.86	2.186	2.384	2.52-2.78, [18]
	25.257	27.739	45.714	47.289	0.86	2.354		
	25.489	28.158	45.786	47.579	0.86	2.619		
Soil	25.237	27.406	45.769	47.134	0.86	2.319	2.564	2.55-2.60, [17]
	25.319	27.213	45.709	47.000	0.86	2.692		
	25.257	27.384	45.727	47.172	0.86	2.682		

To calculate the density of the liquid-solid mixture of concentration 2%, 4%, 6%, 8% and 10%, the calculation formula was used:

$$\rho_s = \frac{m}{V}\ (\mathrm{kg/m^3}) \tag{6.10}$$

where ρ_s represents the density of the liquid-solid mixture, (g/cm^3); m – suspension mass, (g); V – suspension volume, (cm^3).

A graduated cylinder with a known volume of 50 cm^3 was used, the mass of solid particles corresponding to the five concentrations being 1 g, 2 g, 3 g, 4 g, 5 g. The experimental results are presented in Table 6.17.

Table 6.17. The experimental results obtained for the density of the three types of liquid-solid mixture, of known concentrations

Type of material	c, %	ρ_S, g/cm^3		c, %	ρ_S, g/cm^3		c, %	ρ_S, g/cm^3
Calcium carbonate	2	1.011	Blue clay	2	1.014	Soil	2	1.006
	4	1.016		4	1.036		4	1.019
	6	1.023		6	1.047		6	1.024
	8	1.045		8	1.059		8	1.041
	10	1.067		10	1.063		10	1.060

The viscosity of the three liquid-solid mixtures, for each concentration, was measured using the Hoppler ball viscometer and was determined using the relation:

$$\eta = \frac{2}{3}\cdot\frac{(\rho_2-\rho_S)\cdot g\cdot r^3}{d^2}\cdot t\cdot ln\frac{R}{r} = k\cdot(\rho_2-\rho_S)\cdot t \tag{6.11}$$

where ρ_2 – ball density, (kg/m^3); ρ_s – suspension density, (kg/m^3); g – gravitational acceleration, (m/s^2); r – radius of the tube, (m); R – ball radius, (m); d – the diameter of the ball, (m); t – time, (s); k - the constant that characterizes the device and the ball used. The experimental results obtained are presented in Table 6.18.

Table 6.18. The experimental results obtained for the viscosity of the three types of liquid-solid mixture, of known concentrations

Type of material	c, %	t, s	η, mPa·s		c, %	t, s	η, mPa·s		c, %	t, s	η, mPa·s
Calcium carbonate	2	2.54	2.101	Blue clay	2	2.76	2.282	Soil	2	2.72	2.252
	4	2.72	2.249		4	2.80	2.308		4	2.81	2.322
	6	2.78	2.296		6	2.92	2.403		6	2.89	2.386
	8	2.81	2.313		8	2.99	2.457		8	2.99	2.463
	10	2.93	2.405		10	3.08	2.529		10	3.07	2.522

Taking into account that all parameters are known, the experimental data obtained for all three types of liquid-solid mixture, for the five concentrations for each mixture, were used to determine the settling rate, see Table 6.19.

Table 6.19. The experimental results obtained for settling rates, for three types of liquid-solid mixture, of known concentrations

Type of material	c, %	v, m/s		c, %	v, m/s		c, %	v, m/s
Calcium carbonate	2	$1.45\cdot10^{-2}$	Blue clay	2	$1.31\cdot10^{-2}$	Soil	2	$6.03\cdot10^{-2}$
	4	$1.35\cdot10^{-2}$		4	$1.27\cdot10^{-2}$		4	$5.80\cdot10^{-2}$
	6	$1.32\cdot10^{-2}$		6	$1.21\cdot10^{-2}$		6	$5.63\cdot10^{-2}$
	8	$1.29\cdot10^{-2}$		8	$1.17\cdot10^{-2}$		8	$5.39\cdot10^{-2}$
	10	$1.22\cdot10^{-2}$		10	$1.13\cdot10^{-2}$		10	$5.20\cdot10^{-2}$

Based on the experimental results, the curves of variation of the settling rate were plotted, according to Stokes' law, depending on the concentration of solid particles, for each type of liquid-solid mixture (Fig. 6.42).

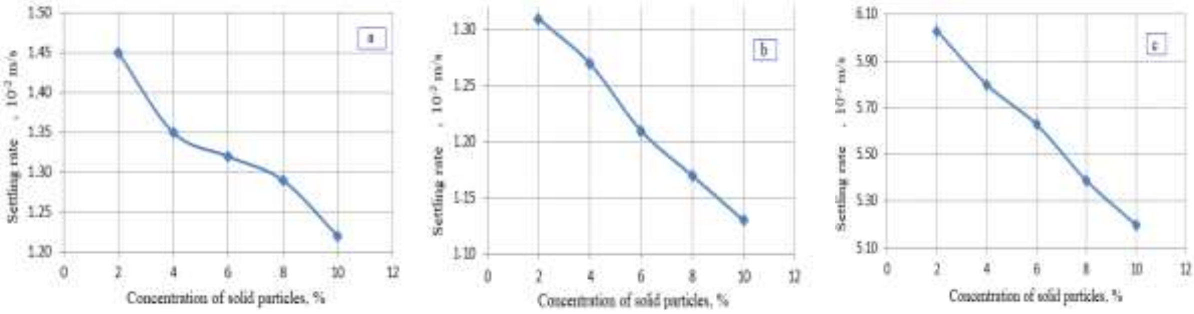

Fig. 6.42. Variation of settling rate depending on the concentration of solid particles, in the case of the suspension water - calcium carbonate (a), water - blue clay (b) and water - soil (c)

According to these variations, it can be noticed that the settling rate is influenced by the concentration of solid particles (the rate decreases as the particle concentration increases), of solid particle size (velocity increases as particle size increases), as well as the density of solid particles (as their density increases, so does the settling rate). The results obtained are in correlation with the results obtained in the literature, [145].

6.3.6. Experimental research on the influence of coagulants on the settling process

For the study of the coagulation flocculation was used the laboratory device W1 (Armfield, UK). The aim of the experiment was to observe the influence of the coagulant on the settling process, measuring the turbidity and color before and after the addition of the coagulant. The coagulant used was aluminum sulphate $Al_2(SO_4)_3$, a solid industrial product, which has the property of producing water clarification.

Five graduated vessels of the apparatus were used for the flocculation study which were filled with 1L of water sample, then the coagulant was dosed, in the first vessel no coagulant was added (vessel control), in the vessel 2 was introduced 1 mL of coagulant, in the vessel 3 was added 2 mL, in the vessel 4, 3 mL and in the vessel 5 were added 4 mL of coagulant.

After mixing for 1 min the coagulant solution from the five vessels (Fig. 6.44), the stirring speed was adjusted to 30 rpm and the mixing time to 20 min and the mixing process was resumed (Fig. 6.45).

Fig. 6.44. Homogenization for 1 minute, [165]

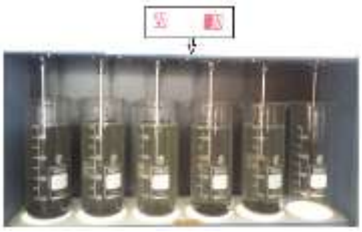

Fig. 6.45. Coagulation after 20 min, [165]

At the end of the determinations, were measured the turbidity and the color of the liquid using a photometer, respectively the pH of the clarified water (supernatant) from each graduated vessel. The results obtained in the coagulation-flocculation process are presented in Table 6.20. Based on these, it was established that the optimal dose of coagulant was 4 mL, the turbidity being reduced by about 8 times.

Table 6.20. The experimental data recorded in the coagulation process, [119]

Vessel	The dosage of coagulant, mL/L	Turbidity, FAU	Color, Hazen	pH
1	0	198	75	9.89
2	1	60	73	9.73
3	2	48	70	9.58
4	3	28	61	9.56
5	4	24	45	9.54

Based on these data, the variations of pH, turbidity and color of the wastewater sample were plotted, depending on the coagulant dose (Fig. 6.46 - 6.48).

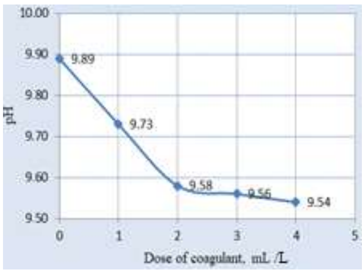

Fig. 6.46. Variation of pH depending on the dose of coagulant used, [165]

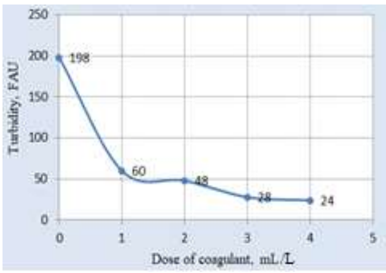

Fig. 6.47. Variation of turbidity depending on the dose of coagulant used, [165]

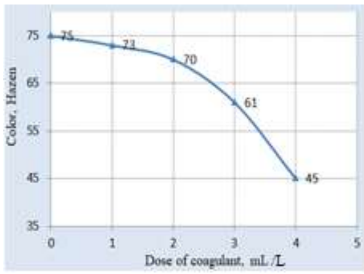

Fig. 6.48. Variation of supernatant color depending on the dose of coagulant used, [165]

Finally, it can be concluded that:

- adding coagulant in water treaty does not significantly affect pH, alkaline character keeping this throughout the experiment (9.54 – 9.89);
- tests conducted showed that as the coagulant dose was increased, the decrease was observed: the turbidity (from 198-24 FAU) and the color (from 75-45 Hazen) of the water sample analyzed, for coagulant doses 0 – 4 mL/L.

6.4. In-situ research on urban wastewater treatment

These researches were carried out in two urban wastewater treatment plants, located in different areas of Romania, stations hereinafter referred to as station A and station B[1].

6.4.1. Experimental determinations regarding the efficiency of a radial clarifier for urban wastewater

The measurements were performed at treatment plant A, provided with two treatment stages, in 2019, at one of the primary radial clarifiers, within the station and aimed to determine the efficiency of the clarifier in a winter month (January), and in a summer month (July). Due to the protocol established with the station management, only general determinations on the efficiency of a radial clarifier regarding the liquid-solid concentration at the outlet of the clarifier, compared to the initial concentration of wastewater at the inlet of the clarifier, were successful. For each day in January and July were recorded the concentrations of impurities (mg/L) at the inlet of clarifiers (c_i) and in the clarified water, at the outlet (c_e), on the basis of which the separation efficiency of the clarifier can be determined *E* (%), using eq. (4.46). The values resulting from the measurements are presented in Table 6.21.

Table 6.21. Values of the inlet and outlet concentration of the clarifier for January and July of 2019

Month January				Month July			
T, ºC	c_i, mg/L	c_e, mg/L	E, %	T, ºC	c_i, mg/L	c_e, mg/L	E, %
≈ 10	157	78	50.32	≈ 22	178	82	53.93
	126	68	46.03		146	76	47.95
	224	80	64.29		156	80	48.72
	258	100	61.24		166	66	60.24
	200	98	51		180	86	52.22
	160	86	46.25		260	90	65.38
	141	82	41.84		164	96	41.46
	175	84	52		254	78	69.29
	221	104	52.94		184	52	71.74
	189	78	58.73		218	58	73.39
	198	82	58.59		150	76	49.33
	372	112	69,89		134	78	41.79
	280	90	67.86		208	94	54.81
	182	84	53.85		156	86	44.87
	190	86	54.74		142	82	42.25
	172	96	44.19		236	82	65.25
	202	82	59.41		180	100	44.44
	284	80	71.83		170	82	51.76
	196	78	60.2		172	90	47.67
	194	88	54.64		274	92	66.42
	343	98	71.43		136	80	41.18
	218	100	54.13		190	86	54.74
	220	102	53.64		198	72	63.64
	178	114	41.57		200	72	64
	258	99	61.63		156	76	51,28
	184	88	52.17		276	86	68.84
	166	70	57.83		164	88	46.34
	208	96	53.85		182	68	62.64
	188	104	44.68		182	66	63.74
	224	116	48.21		278	68	75.54
	194	106	45.36		198	74	62.63

[1] The data were determined in existing urban wastewater treatment plants, but are part of a confidentiality protocol established with the management of the treatment plants.

The data were processed with the M. Excel program, graphically representing the variation of efficiency during the 31 days, both for January and for July (Fig. 6.51). It can be sobserved that if the value of the concentration of solid particles is higher, the efficiency of the settling process also increases (> 60%). The higher values of the inlet concentration of clarifier are due to more abundant precipitation, but also to uncontrolled discharges. The efficiency of January was 54.98%, and the efficiency of July was 56.37%. Figure 6.52 shows the efficiency variation for each month of 2019, the efficiency of the clarifier in 2019, based on the recorded data being 48.85%.

Table 6.22. The values of the monthly averages for the concentration of inlet, outlet of the clarifier and its efficiency

Month	Monthly average concentration c_i, mg/L	Monthly average concentration c_e, mg/L	Monthly efficiency of the clarifier E,%
January	209.74	91.26	54.98
February	198.6	110.3	44.46
March	215.3	118.5	44.96
April	248.14	127.4	48.66
May	233.22	117.9	49.45
June	210.74	108.5	48.51
July	189.94	79.42	56.37
August	184.28	96.3	47.74
September	196.87	99.4	49.51
October	224.23	115.7	48.40
November	200.2	106.76	46.67
December	230.42	123.41	46.45

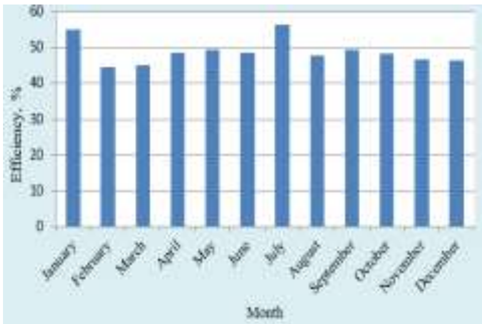

Fig. 6.52. The efficiency of the settling process for the months of 2019

From what it is presented, it is observed that there is not necessarily a correlation of the efficiency of the clarifier with the atmospheric temperature, although the average efficiency during the summer months is slightly higher than for the months with lower temperature. It is very likely, as already mentioned, that this is due to the fact that there was no strict record of the amounts of precipitation that fell in those months, especially because the months with higher temperatures (April - October) had a rainfall deficit.

6.4.2. Experimental determinations on the removal by sieving (screening) of solid wastes in municipal wastewater

In the sieving installations of treatment plant A, which have in structure rare bar screens (Fig.6.53a) and dense bar screens (Fig. 6.53b), arranged successively, a quantity of coarse suspensions of approx. 5 - 6.5 t/day (these are placed at the front of the mechanical stage of the treatment plant in order to retain and discharge the coarse suspensions from the wastewater subjected since the beginning of the technological process in order to protect and properly operate the treatment plant). The composition of the waste from the screening is as follows: textile materials - approx. 60%; plastics - approx. 25%; vegetable waste - approx. 10%; paper - 5%. At wastewater treatment plant A, this impressive amount of waste from screening plants is collected as such in eurocontainers, without being subjected to other specific treatments (*dehydration and compaction)*, being subsequently transported to solid waste landfills with significant costs.

a b

Fig. 6.53. The material from the wastewater treatment screening plant

In this sense, in 2017 an innovative technology was proposed for processing waste from screening plants, which was implemented and built at the treatment plant with important benefits. Figure 6.54 shows the diagram of the technological flow of the waste processing technology coming from the sieving installations of the wastewater treatment plant A.

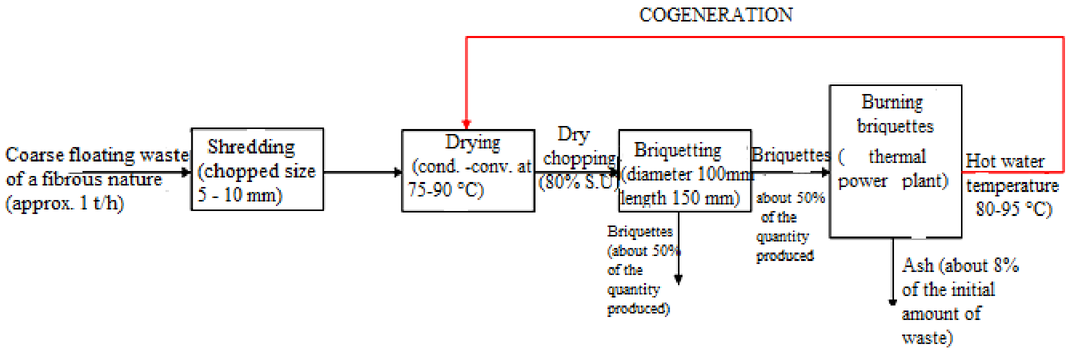

Fig. 6.54. Scheme of the technological flow of waste treatment from the sieving installations of the wastewater treatment plant A

Six samples of waste were taken for analysis, taken at intervals of one week from the retained waste storage container. The initial density of the samples was determined using a cubic box with a side of 0.2 m, by weighing them. Subsequently, material samples were subjected to the following operations:

a) The shredding of the waste material was done with equipment consisting of two horizontal driven rotors, provided with cutting blades (Fig. 6.56a). After shredding, a material wtith particle sizes between 5 - 10 mm has resulted (Fig. 6.56b).

a b

Fig. 6.56. Shreddings rotors fitted with cutting blades (a) and the appearance of the resulting shredding (b)

b) Drying of the shredded material was performed in a dryer with multi-layered platters (hearths) in which the drying process took place by conduction and convection at a temperature of 75-90 °C**.** Thus, the material resulting from the shredding was deposited on the upper platter, from where it was taken and moved along it, then discharged on the next, so that the process was repeated successively until the material went through all the platters of the dryer (Fig. 6.58). The heating agent that heated the platters was hot water, obtained by cogeneration within the proposed technology.

c) Briquetting of shredded and dried material was performed by mechanical pressing in hydraulic piston press (Fig. 6.59). It is mentioned that this variant was chosen because the humidity of the briquetting material is 20%, optimal for this type of equipment.

Fig. 6.58. Dryer with multi-layered platters (hearths)

Fig. 6.59. Hydraulic press with piston for briquetting

The briquettes obtained had a diameter of 100 mm and a length of approx. 150 mm. The appearance of the briquettes obtained experimentally by this process is shown in Fig. 6.60.

Fig. 6.60. The appearance of the briquettes obtained

d) The burning of the briquettes in order to obtain a thermal agent for the cogeneration of the drying is carried out in a thermal power plant with excess air.

For the six samples, the variation of the initial and final density was made (Fig. 6.62). From the graph in Fig. 6.62 it is observed that the density of the six samples of waste coming from the sieving installations of the wastewater treatment plant A decreased proportionally for each sample, the average amount of wastewater discharged after drying being 166 L/m^3.

Table 6.23. The experimental results obtained in the case of the six samples of waste from the sieving plants of the wastewater treatment plant A

Waste screens structure	Specific gravity (after measurements), kg/m^3				Residual water quantity
	Initial		Final (after drying)		
	Density, kg/m^3	Humidity, %	Density, kg/m^3	Humidity, %	%
Sample 1	582	39	408	13	174
Sample 2	542	40	383	15	159
Sample 3	568	39	403	14	165
Sample 4	593	41	417	16	176
Sample 5	531	39	372	13	159
Sample 6	556	38	392	12	164
Total average samples	562	39	396	14	166

It should be mentioned that the reduction of the material humidity decisively influences the value of the caloric power of the briquettes obtained later. In the platters dryer the humidity of the material was reduced from approx. 65%, as it initially had, at approx. 20%, value imposed by the subsequent briquetting phase (Fig. 6.63).

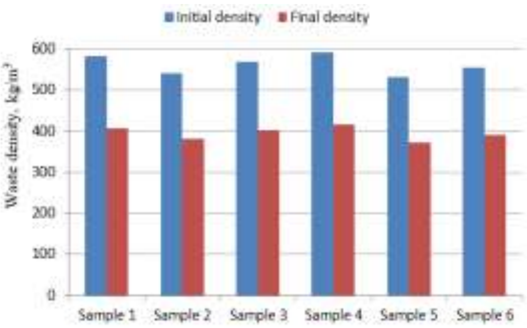

Fig. 6.62. The initial and the final density of the six samples of waste sieving from the wastewater treatment plant A

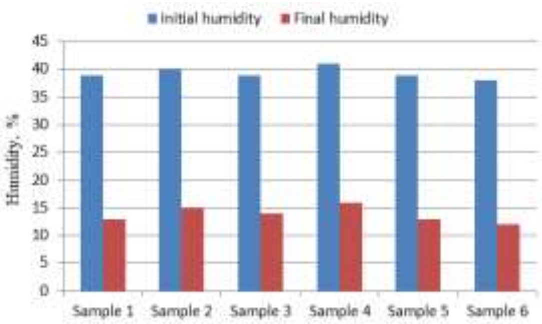

Fig. 6.63. The initial and the final humidity of the six samples of waste sieving from the wastewater treatment plant plant A

The quantity of briquettes generated following the processing of waste from the wastewater treatment plant screening facilities is presented in Table 6.24. For the production of the thermal agent necessary for drying, a part of the obtained briquettes is used, the rest being used for sale.

Table 6.24. The quantity of briquettes generated from the processing of waste sieving from the wastewater treatment plant A

Internal consumption of briquettes in the technological process of processing		
Gross quantity of waste processed per month = 174 t	kg briquettes / m^3 processed waste	total quantity of briquettes obtained t/month
The quantity of briquettes produced	396	124
The quantity of briquettes consumed for waste treatment	38	12
The quantity of briquettes left for sale	358	112

Given the inhomogeneous composition of briquettes with significant influences on their calorific value, it is necessary an ***automatic cogeneration control system*** that involves regulating the required temperature of the drying agent by automatically changing the parameters of the thermal power plant, such as: briquette feed rate and air flow necessary for combustion *(this is studying a patent with no. registration OSIM: a 201701031/05.12.2017, annex A.6.3)*, [38].

6.4.3. Determination of the amount of waste retained by screening plants and the total content of suspended solids

The determinations were carried out in a wastewater treatment plant B with a capacity to treat an average daily flow of 2550 m^3/day (107 m^3/h), with the capacity of a maximum flow in dry weather of 195 m^3/h, respectively 343 m^3/h maximum flow in rain. The treatment plant serves a population of approximately 11,100 equivalent inhabitants, being developed on two technological treatment lines (a mechanical stage and a biological stage).

The treatment plant is equipped with two rare bar screens (with a distance between bars of 40 mm) and two dense bar screens (with a distance between bars of 6 mm), mounted in two reinforced concrete channels. Both types of bar screens are 0.7 m wide and are mounted at an angle of 70 ^{o} (Fig. 6.65). The waste retained by means of sieving plants is reprezented by textiles, plastics, vegetable waste and paper.

Fig. 6.65. Dense bar screens (a), respectively rare (b) from the structure of the urban wastewater treatment plant

In this study, were determined the quantities of coarse material (by weighing), retained from the treatment plant using the two types of bar screens, the determinations being carried out for two winter months of 2020 (January and February), but also for three months with higher temperatures of the same year (July - September). The results are presented in Table 6.25.

Based on these determinations, was pltted the variation of the quantities of coarse waste retained with the help of the rare and dense bar screens from the municipal wastewater treatment plant, for the five months (Fig. 6.66).

Also in the treatment plant B were determined the total suspended matter (MTS), both from the influence and from the effluent of the treatment plant, thus determining the efficiency of the plant in terms of removal of these materials.

Table 6.25. The quantity of waste retained by dense and rare bar screens in the treatment plant, including their operating hours

Equipment type	The month of determinations	Retained waste, kg	Influent flow, m^3/lună	Total working hours, h
Dense and rare	January	300	22685	7.25
	February	200	21049	6.5
	July	400	19747	7.5
	August	400	19523	5.5
	September	600	18408	5

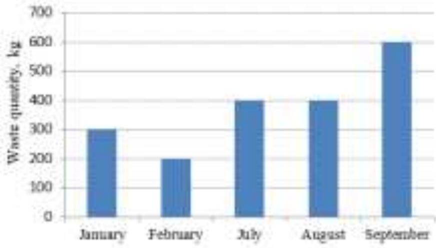

Fig. 6.66 The quantity of waste retained by dense and rare bar screens in the treatment plant

The quantity of solids was determined using the relationship:

$$MTS = \frac{m_2 - m_1}{V} \cdot 1000\ (mg/L) \quad (6.12)$$

where m_1 represents the mass of the filter paper, (g); m_2 – mass of filter paper with solid particles, (g); V- the volume of wastewater analyzed, (L).

These steps were performed for both the influent and the effluent of the treatment plant for the five months analyzed. The experimental results are presented in Table 6.26.

Table 6.26. The experimental results in terms of total suspended solids content in the effluent and effluent of the treatment plant for the five months

Month	Influent flow, m^3/month	MTS influent, mg/L	MTS authorized, mg/L	MTS effluent, mg/L	Plant efficiency, %
January	22685	297	35 mg/L	5,5	98.15
February	21049	297		5	98.82
July	19747	768		6	99.22
August	19523	872		4,8	99.45
September	18408	525		5,5	98.95

Based on these results, were plotted the variation curves of the total content of suspended matter for the influent and effluent of the urban wastewater treatment plant (Fig. 6.67). It can be observed that in all five months the quantities of suspended matter was significantly reduced, each month falling within the permissible limits for this parameter analyzed, the efficiency of the treatment plant being in this case higher than 98% for all five months (Fig. 6.68).

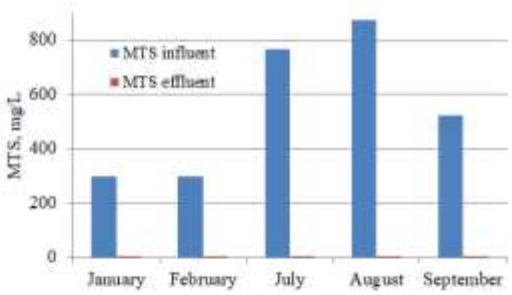

Fig. 6.67. Total suspended solids content, for the influent and effluent from treatment plant B, for all the five months analyzed

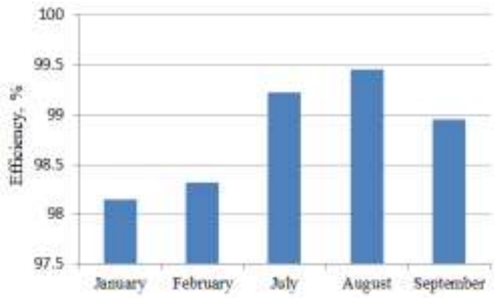

Fig. 6.68. The efficiency of the treatment plant for the total content of suspended matter, for all the five months analyzed

6.5. Conclusions

If the concentration of the suspension is lower, the settling process takes place faster, and as the concentration of particles increases, so does the time required to remove them from wastewater because their settling rate decreases.

In the case of the determining the clarification curve of aqueous suspensions of solid particles, using the intelligent Raspberry Pi, the turbidity value in the 80 minutes in which the measurements were made, for the height of 75 mm decreased from 260 NTU to approx. 11 NTU, for the height of 65 mm the turbidity had values between 222 and 13 NTU, and for the height of 55 mm, the turbidity had variations from 246 to 26 NTU.

The density of the six samples of waste coming from the sieving installations of the wastewater treatment plant A decreased proportionally for each sample, the average amount of wastewater discharged after drying being 166 L/m^3, and the efficiency of the treatment plant B it was higher than 98% for all five months analyzed.

CHAPTER 7. FINAL CONCLUSIONS. PERSONAL CONTRIBUTIONS. RECOMMENDATIONS AND PERSPECTIVES FOR FUTURE RESEARCH

7.1. General conclusions on theoretical and experimental aspects

1. The process of separating the liquid-solid mixture is influenced by numerous factors related to the solid component, the liquid component and at the constructive factors of the equipment used for this purpose;

2. Settling is of particular importance in wastewater treatment, in which case the tailings ponds can represent as much as 30% of the investments in a treatment plant;

3. The experimental research conducted for the purpose of determination the settling rate is influenced by the concentration of solid particles (the rate decreases as the particle concentration increases), of solid particle size (velocity increases as particle size increases), as well as the density of solid particles (as their density increases, so does the settling rate).

7.2. Personal contributions

1. Synthetic analysis of the literature on the current state of theoretical and experimental research conducted in the field of wastewater settling process, by consulting a number of 226 papers published internally and internationally;

2. Development an algorithm based on experimental data, using the program MathCad, for determining the position of the critical point of the clarification curve at the sedimentation of solid particles in stationary column;

3. Numerical CFD simulation of the settling process in the case of two constructive variants of decanters, in order to determine the optimal constructive variant;

4. Carrying out experimental research on the influence of solid particle concentrations on the settling process, for three types of suspensions in order to determine their clarification curves;

5. Carrying out experimental research in order to calculate the settling rate for the three types of suspensions, previously determining experimentally the density of solid particles, the density and viscosity of the suspension;

6. Determination of the clarification curve of an aqueous suspension of solid particles, using the intelligent Raspberry Pi system by processing the images of the separation interface between the clarified area and the suspension area with solid particles in full settling process;

7. Expressing a set of conclusions and recommendations that can be useful for further research in the field;

8. Carrying out in-situ experimental research within the urban treatment plants in order to capitalize on the coarse impurities, retained by the screening facilities;

9. Determining of the suspended matter content of the influent and effluent of an urban wastewater treatment plant;

10. The results obtained in the studies and research carried out in the thesis were capitalized by the elaboration and publication of a number of 12 scientific papers in specialized journals, in volumes of national and international conferences and their presentation at national and international scientific events, in as author and co-author (of these 2 being ISI indexed).

7.3. Recommendations and perspectives for future research

From the analysis of experimental data and own research can be made the following recommendations:

1. It is necessary a mathematical modeling of the process of settling solid suspensions in wastewater taking into account as many process parameters as possible, in order to identify the correlation between them and the influence on the efficiency of the process, but also on the equipment used;

2. In order to increase the efficiency of the process of settling of solid particles in the liquid-solid mixture, it is recommended to use radial settlers with a central supply pipe of constant diameter up to a certain height after which it should be flared to a larger diameter so that the water supply in the clarifier to have a linear flow, without eddy currents affecting the settling;

3. Regardless on the type of clarifier used, it is important to be able to take liquid samples at depth, in order to analyze the turbidity and concentration of solid particles, but also the temperature of the liquid, knowing that the temperature affects both viscosity and settling process, this is highlighted by determining the efficiency of clarifiers in winter and summer months;

4. For the treatment of coarse waste retained by mechanical methods (sieving) from wastewater in treatment plants, it is recommended to use the technology presented in the thesis, in order to recover this waste in the form of fuel briquettes.

For future research, the following may be recommended:

1. Research on the influence of fluid temperature on the settling process in longitudinal and radial clarifiers;

2. Research on the influence of wastewater flow on the settling process in radial clarifiers;

3. Research on settling rate in horizontal settlers according to fluid velocity at inlet and the solids concentration;

4. Research on the influence of mixtures of raw materials of different sizes on the settling process in stationary columns;

5. Performing experiments on an experimental model of clarifier, designed according to the characteristics of the one used in the simulation in the thesis.

SELECTIVE REFERENCES

[1] *Adams E.W., Rodi, W.*, Modelling flow and mixing in sedimentation tanks, J. Hydraul. Eng., vol. 116, no. 7, 1990, pp. 895–911.

[2] *Adams N.W.H., Kramer J.R.*, Silver speciation in wastewater effluent, surface waters, and pore waters, Environ. Toxicol. Chem., vol. 18, no. 12, 1999, pp. 2667-2673.

[3] *Al-Baidhani J., Salih H.*, Effects of Shape and Dimensions of Plain Sedimentation Basins, J. Eng. Appl. Sci., vol. 13, 2018, pp. 10730-10734.

[4] *Al-Jeebory A.A, Kris J., Ghawi J.H.*, Performance improvement of water treatment plants in Iraq by CFD model, QJES, vol. 3, no. 1, 2010, pp. 1-13.

[5] *Amvrossios C.B, Atmadja J.*, Mathematical Methods for Hydrologic Inversion: The Case of Pollution Source Identification, Handb. Environ. Chem. Vol.5, Part F, vol. 3, 2005, pp. 65–96.

[6] *Anastasiu D.*, Water distribution and wastewater disposal, in 2018, National Institute of Statistics, 2019.

[7] *Andral M.C., Roger S., Montréjaud-Vignoles M., Herremans L.*, Particle size distribution and hydrodynamic characteristics of solid matter carried by runoff from motorways, Water Environ. Res., vol. 71, no. 4, 1999, pp. 398-407.

[8] *Anjum M.N., Rasheed H.U., Ahmed W.*, Impact of Waste Water Treatment on Quality of Influent & Effluent Water, IJIR, vol. 2, nr.11, 2016.

[9] *Antoniu, R., Negulescu C.*, Industrial wastewater treatment, vol.1 and 2. Technical Publishing House, Bucharest, 1987.

[10] *Aguilar M.I., Saez J.*, Improvement of coagulation-flocculation process using anionic polyacrylamide as coagulant aid, Chemosphere, vol. 58, 2005, pp. 47-56.

[11] *Albertson O.*, Clarifier Design, in Design and Retrofit of Wastewater Treatment Plants for Biological Nutrient Removal, Randall, C. et al., editors, Technomic Publishing Co., Lancaster, Pennsylvania, 1992.

[28] *Cîrţînă D.*, Wastewater treatment, Academica Brâncuşi, Târgu Jiu, 2007.

[29] *Coldea S., Ionescu Gh.C.*, Elements of fluid physics and hydraulics. Matrix Rom Publishing House, Bucharest, 2005.

[30] *Corey A.T.*, Influence of Shape on the Fall Velocity of Sand Grains, Colorado State University, Fort Collins, Masters Thesis, 102 p. 1949.

[48] *Ghawi A.H., Kriš J.,* A Computational Fluid Dynamics Model of Flow and Settling in Sedimentation Tanks, Applied Computational Fluid Dynamics, chapter 2, Croația, pp. 19-34, 2012.

[49] *Ghawi A.H., Kriš J.,* Improvement performance of secondary clarifiers by a computational fluid dynamics model. SJCE, vol. 19, nr. 4, 2011, pp. 1–11.

[50] *Ghawi A.H., Kriš J.,* A numerical model of flow in sedimentation tanks in Slovakia, AKJournals, vol. 3, nr. 2, 2008, pp. 59-73.

[82] *Machado V.C., Gabriel D., Lafuente J., Baeza J.A.*, Cost and effluent quality controllers design based on the relative gain array for a nutrient removal WWTP, Water Res., vol. 43, no. 20, 2009, pp. 5129–5141.

[83] *Mackenzie L.D.*, Water and Wastewater Engineering: Design Principles and Practice, McGraw-Hill, 2010.

[84] *McCorquodale J.A*, Temperature profiles in primary settling tanks, IRI Report University of Windsor, Canada, 1977.

[85] *McNown J.S., Lin P.N.*, Sediment concentration and fall velocity. Proc. 2nd. Midwest. Conf. Fluid Mech., Ohio State Univ., 1952, pp 401-411.

[86] *Medina V.M.E.,* Secondary settling tanks modeling: study of the dynamics of activated sludge sedimentation by computational fluids dynamics, PhD Thesis, Chemical and Process Engineering, Université de Strasbourg, 2019.
[96] *Panaitescu M.,* Wastewater treatment techniques. Treatment plant design guide, Nautical Publishing House, 2011.
[97] *Parry A.,* Numerical Simulations and Optimisation of Gas-Solid-Liquid Separator, MSc Thesys in Petroleum Engineering, Imperial College London, 2014.
[98] *Păun M.C.,* Studies and research on high-performance clarification technologies in drinking water production, PhD thesis, Technical University of Constructions Bucharest, 2011.
[99] *Podoleanu C.E.*, Contributions to the treatment plants to optimize operation, PhD. Thesis, U.P.Timişoara, 2006.
[100] *Podoleanu C.E.*, Optimization of the longitudinal horizontal settling tanks exploitation within a drinking surface water stations, Buletinul Ştiinţific al Universităţii "POLITEHNICA" din Timişoara, vol. 55, no. 69, Fascicola 2, 2010.
[101] *Podolsky R.D.,*Temperature and water viscosity: Physiological versus mechanical effects on suspension feeding, Science, vol. 265, no. 5168, 1994, pp. 100-103.
[124] *Safta V.V., Dincă M., Constantin G-A.,* ***Zăbavă B-Ş.,*** Critical point determination of the clarifying curve of aqueous diluted suspensions, ATAE, vol. 45, 2017, pp. 99-110.
[125] *Safta V.V., Toma M. L., Ungureanu N.,* Experiments in the field of water treatment, PRINTECH Publishing House, Bucharest, 2012.
[163] ***Zăbavă B.Șt.****, Constantin G.A., Voicu Gh.,* Numerical CFD analysis in a radial decanter. The Scientific Bulletin of the Polytechnic University of Bucharest, 2020 (accepted for publication).
[164] *Zăbavă B.Șt., Ipate G., Voicu Gh., Dincă M., Ungureanu N., Ferdeş M., Vlăduţ V.,* Smart system to monitor water treatment based on Raspberry PI computer, ATAE, vol. 47, 2019, pp. 159-166.
[165] ***Zăbavă B.Șt****., Ungureanu N., Vlăduț V., Dincă M., Voicu Gh.* Experimental study of coagulation – flocculation process of fine and colloidal impurities in a river from Nehoiu, Romania, Development Directions of Tractors and Renewable Energy Resources, vol. 21, no. 1, 2016, pp. 80-86.
[166] ***Zăbavă B.Șt.,*** *Voicu Gh., Dincă M., Ungureanu N., Ferdeș M.,* Factors that influence the efficiency of the decanting process – a review, TE-RE-RD, vol. 7, 2018, pp. 423-426.
[167] ***Zăbavă B.Șt.,*** *Voicu Gh., Safta V.V., Ungureanu N., Dincă M., Ionescu M., Munteanu M., Ferdeș M.,* Considerations on the equipment used for wastewater settling – a review, ISB-INMA TEH - Agricultural and Mechanical Engineering, Bucharest, 2016, pp. 561-566.
[169] ***Zăbavă B.Șt.,*** *Voicu Gh., Ungureanu N., Dincă M., Safta V.V.,* Basic equipment for the mechanical treatment of wastewater, ISB-INMA TEH, Agricultural and Mechanical Engineering, 2015, pp. 349-356.
[170] *Zârnoianu D., Popescu S., Brăcăcescu C.,* Theoretical and experimental research on the separation process of impurities from waste water through decantation, COMEC, vol. 6, 2015, pp. 183-190.
[172] *** ANALYSIS TOOLS, ANSYS Advantage, vol. 2, no. 4, 2008.

LIST OF WORKS IN THE FIELD OF THE DOCTORAL THESIS

As.drd.ing. ZĂBAVĂ Bianca – Ștefania

1. **Zăbavă B.Șt**., Constantin G.A., Voicu Gh., *Numerical CFD analysis in a radial decanter*. Scientific Bulletin of the Polytechnic University of Bucharest, 2020 (accepted for publication, SCOPUS)
2. **Zăbavă B.Șt**., Ipate G., Voicu Gh., Dincă M., Ungureanu N., Ferdeş M., Vlăduţ V. *Smart system to monitor water treatment based on Raspberry PI compute*r. „Actual Tasks on Agricultural Engineering”, 5–7 March 2019, Vol. 47, pp. 159-166, Croaţia, Opatija, ISSN 1848-4425. WOS:000472729500015

3. V.V. Safta, M. Dincă, G-A. Constantin, **B-Ş. Zăbavă**, *Critical point determination of the clarifying curve of aqueous diluted suspensions*. "Actual Tasks on Agricultural Engineering", Vol. 45, Opatija, Croaţia, 21-24 feb. 2017, pp. 99-109, ISSN 1848-4425, WOS:000432420200010
4. George Ipate, Gabriel Musuroi, Gabriel-Alexandru Constantin, Elena Madalina Ştefan, **Bianca Zăbavă** and Marina Pihurov, *Experimental and numerical simulation research of sedimentation process in stationary column of aqueous suspension of solids*, 8th International Conference on Thermal Equipment, Renewable Energy and Rural Development (TE-RE-RD 2019), https://doi.org/10.1051/e3sconf/201911203028 (SCOPUS)
5. **Zăbavă B.Șt**., Voicu Gh., Ungureanu N., Vlăduț V., Dincă M., Ionescu M. *Experimental study of the sedimentation of solid particles in wastewater.* Scientific International Conferences – The 12th Annual Meeting „Durable Agriculture – Agriculture of the Future", Craiova. Annals of the University of Craiova – Agriculture, Montanology, Cadastre Series. Vol. XLVI/2, Working group no. 4 – Management, Agriculture Mechanization and Cadastre, 17-18 Nov. 2016, pp. 611-617, ISSN 1841-8317, (BDI: CAB Abstracts– CNCSIS category B+).
6. **Zăbavă B.Șt.,** Voicu Gh., Safta V.V., Ungureanu N., Dincă M., Ionescu M., Munteanu M., Ferdeș M. *Considerations on the equipment used for wastewater settling – a review*. International Symposium ISB-INMA TEH - Agricultural and Mechanical Engineering, pag. 561-566, 27-29 oct. 2016, Bucharest. ISSN 2537-3773, (BDI – CABI).
7. **Zăbavă B.Șt**., Voicu Gh., Ungureanu N., Dincă M., Ionescu M., Munteanu M., Pruteanu A. *Consideration on the constructive factors of clarifiers and their influence on the settling process efficiency – a review*. 6th International Conference on Thermal Equipment, Renewable Energy and Rural Development (TE-RE-RD), 8-10 June 2017, Moieciu de Sus, România pp. 295-300, ISSN 2457-3302, [BDI: Index Copernicus International, EBSCO Publishing Databases].
8. **B.Șt. Zăbavă**, Gh. Voicu, M. Dincă, N. Ungureanu, M. Ferdeș. *Factors that influence the efficiency of the decanting process – a review. 7th* International Conference on Thermal Equipment, Renewable Energy and Rural Development (TE-RE-RD), Drobeta Turnu Severin – Romania 31 mai - 02 Junie 2018, pp. 423-426, ISSN 2457 – 3302, [BDI: Index Copernicus International, EBSCO Publishing Databases].
9. **Zăbavă B.Șt**., Voicu Gh., Ungureanu N., Dincă M., Ferdeș M., Safta V.V., Ipate G. *Study of water turbidity determination using standard samples*. Proceedings of 6th International Conference „Research People and Actual Tasks on Multidisciplinary Sciences", pp. 124-128, ISSN 1313-7735, Printing House "Angel Kunchev" University of Ruse, 12 – 15 June 2019, Lozenec, Bulgaria [BDI: CABI].
   http://conf.bionetsyst.com/wp-content/uploads/2019/12/Volume1-Lozenec-2019.pdf
10. **Zăbavă B.Șt.,** Ungureanu N.,Vlăduț V., Dincă M., Voicu Gh. *Experimental study of coagulation – flocculation process of fine and colloidal impurities in a river from Nehoiu, Romania.* The XXIII Scientific Meeting „Development Directions of Tractors and Renewable Energy Resources". Tractors and driving machines (Traktori I Pogonske Masine) 1, ISSN 0354-9496, vol. 21, no. 1/2016, December 2016, Novi Sad, Serbia. pp. 80-86.
11. **Zăbavă B.Șt**., Voicu Gh., Ungureanu N., Dincă M., Safta V.V. *Basic equipment for the mechanical treatment of wastewater*. International Symposium ISB-INMA TEH, Agricultural and Mechanical Engineering, 29-31 oct. 2015, Bucharest pag. 349-356,. ISSN 2344-4118. http://isb.pub.ro/isbinmateh/2015/Volume_Symposium_2015 .pdf
12. Duțu I., Safta V.V., Voicu Gh., **Zăbavă B.Șt.,** *Automatic temperature control system of the trays of a conduction-convection dryer, Patent application, Nr. registration* OSIM: a 2017 01031/05.12.2017.

Curriculum Vitae	
Personal information	
Name / Surname	**ZĂBAVĂ Bianca - Ștefania**
Adress	Str. Solstiţiului, no.8, bl. 1, ap 23, city Popești – Leordeni, jud. Ilfov
E-mail	bianca.dragoiu@upb.ro
Birth day	7 iulie 1990
Professional Experience	
Period	Noiembrie 2015 - present
Occupation or position held	University assistant
Main activities and responsibilities	- teaching seminars; - guidance of practical laboratory activities - scientific research activity;
Employer name and adress	University POLITEHNICA of Bucharest, Faculty of Biotechnical Systems Engineering, str. Splaiul Independentei no. 313, corp D, sector 6.
Type of business or sector	Education and research
Period	November 2014 – October 2015
Occupation or position held	Save Desk Rezidential – call center
Main activities and responsibilities	- solving customer complaints - activation / abolition of fixed / mobile services
Employer name and adress	Telekom Romania, Piața Presei Libere, nr 3- 5, sector 1, Bucharest
Type of business or sector	Telecomunications
Education	
Period	October 2015 -present
Qualification / received diploma	Ph.D Student
Name and type of educational institution / training provider	University POLITEHNICA of Bucharest, Faculty of Biotechnical Systems Engineering
Period	2013 – 2015
Qualification / received diploma	Master's degree, Specialization Engineering and Management in Environmental Protection
The main disciplines studied / acquired professional competencies	- Air Quality Engineering - Ecological impact assessment
Name and type of educational institution / training provider	University POLITEHNICA of Bucharest, Faculty of Biotechnical Systems Engineering
Period	2009 - 2013
Qualification / received diploma	Bachelor's degree in engineering, Specialization in Biotechnical and Ecological Systems Engineering
The main disciplines studied / acquired professional competencies	- Environment protection - Depollution systems
Name and type of educational institution / training provider	University POLITEHNICA of Bucharest, Faculty of Biotechnical Systems Engineering
Personal skills and competences	
Native language	**Romanian**
Known foreign language (s)	**English**

Autoevaluation	**Understanding**				**Speaking**				**Writting**	
European level (*)	Listening		Reading		Conversational skills		Oral speech		Written experience	
English	B2	Independent user	B2	Independent user	B1	Independent user	B1	Independent user.	B1	Independent user

(*) Foreign European languages reference level